J Mater Sci (2010) 45:3109–3135
DOI 10.1007/s10853-010-4279-9

REVIEW

Materials and manufacturing technologies for solid oxide fuel cells

Norbert H. Menzler · Frank Tietz · Sven Uhlenbruck · Hans Peter Buchkremer · Detlev Stöver

Received: 7 December 2009 / Accepted: 25 January 2010 / Published online: 17 February 2010

Abstract This article summarises recent developments in solid oxide fuel cell research regarding materials, processing and microstructure–property relationships. In the materials section, the various cell and stack materials are briefly described, i.e. electrolytes, electrodes, contact and protective layers, interconnects and sealing materials. The section on processing gives an overview of manufacturing technologies for cells including a view of different substrate materials and designs. Besides the widely used planar cell designs, the technologies for tubular designs are also described. In addition, the technologies are grouped with respect to the support, e.g. metal- or ceramic–metal (cermet anode substrate)-supported SOFCs. Finally, special emphasis is laid on the microstructure of functional layers which primarily govern the power output of the SOFC.

Introduction

In the last 20 years, research in the field of solid oxide fuel cells (SOFCs) has increased exponentially. This research was promoted by the various advantages which SOFCs have in comparison to other traditional or novel energy devices. Besides their high theoretical efficiency, their possibility of using either natural gas, biogas or methane as fuel (fuel flexibility), their noiseless operation, and, compared to other fuel cells, their operation without using noble metals as catalysts, mention must also be made of the wide variety of possible applications ranging from combined heat and power plants (hundreds of kW) to household energy supply or auxiliary power units for passenger cars or trucks (1–5 kW level).

However, up to now, market entry has not started due to two major drawbacks: first, the costs of components, stacks and systems, and secondly the lack of field tests to ensure reliability with respect to operational conditions like current load and thermal cycles.

R&D in the field of SOFCs has so far dealt with materials development for the cells themselves, the interconnects and the sealing, the manufacturing technologies of cells and interconnects, the introduction of cells into stack designs, proper stack sealing, the balance-of-plant components (reformer, heat exchanges, blowers etc.) and system evaluation including modelling activities with respect to gas flow, heat distribution, and efficiency depending on the various cell architectures and stack designs.

Solid oxide fuel cells (SOFCs) can be grouped into tubular and planar designs. Both types can consist of one or several single cells per stacking unit, i.e. on a single tube or in a single layer. Depending on the application, the tubular SOFCs have dimensions from needle-like shapes to lengths of about 1.5–2 m [1, 2] for rapid start-up times and large gross power, respectively. The planar designs can be divided into stacks containing metallic or ceramic interconnect material and cells with thick (electrolyte-supported) or thin (electrode-supported) membranes with thicknesses usually in the range of 150–250 and 5–20 μm, respectively [3, 4]. The size of technologically relevant planar cells varies from 10×10 to 25×25 cm^2 or according to corresponding areas of a circular shape.

The general tendency today to reduce the operating temperature from about 1000 to 500–800 °C is in favour of cell designs with thin electrolytes due to the lower ohmic resistance and hence the higher power density that can be

N. H. Menzler (✉) · F. Tietz · S. Uhlenbruck · H. P. Buchkremer · D. Stöver
Forschungszentrum Jülich, Institute of Energy Research, IEF-1, 52425 Jülich, Germany
e-mail: n.h.menzler@fz-juelich.de

Table 1 Ionic conductivity (σ_i) of different oxygen ion conductors (in S/cm)

Material	σ_i at 800 °C	σ_i at 600 °C
$Zr_{0.85}Y_{0.15}O_{1.93}$ (8YSZ)	5.0×10^{-2}	6.2×10^{-3}
$Zr_{0.80}Sc_{0.19}Al_{0.02}O_{1.90}$ (10ScSZ-Al)	1.2×10^{-1}	1.1×10^{-2}
$Ce_{0.8}Gd_{0.2}O_{1.9}$ (CGO)	6.5×10^{-2}	1.3×10^{-2}
$La_{0.8}Sr_{0.2}Ga_{0.90}Mg_{0.1}O_{3-x}$ (LSGM)	1.1×10^{-1}	1.6×10^{-2}
$La_{10}Si_6O_{27}$	1.7×10^{-2}	8.2×10^{-2}

achieved. Therefore, many developers regard anode-supported cells as the best choice for realising an SOFC operating at reduced temperature [3–5], see Table 1.

The term 'anode supported' was initially introduced to explicitly indicate that in such fuel cells mechanical stability is transferred from the thick, dense electrolyte layer to an even thicker, porous anode (0.5–1.5 mm, i.e. anode substrate) [6, 7]. In recent years, other types of SOFCs have also been developed which have the mechanical support on the anode side, although this is not necessarily the anode substrate. In all these cases, the substrate is always porous to allow gas transport to and from the anode. The materials used for such substrates are metals or alloys [8], composites like the conventional Ni/8YSZ cermet (8YSZ: 8 mol% yttria-stabilised zirconia) or even refractory ceramics [9]. In the case of insulating substrates, they only deliver the fuel gas to the anode, and the current path has to be established along the substrate surface instead of passing it perpendicular to the substrate surface as in the case of electrically conductive substrates. Thermomechanical compatibility is difficult to achieve with metallic substrates, because, on the one hand, they often have higher thermal expansion coefficients than the other cell components and, on the other hand, severe corrosion can occur leading to failure of cell performance.

On the anode substrate, the other cell components are deposited in the sequence anode–electrolyte–cathode. Normally, the coatings are realised by screen printing (SP), slurry coating, wet powder spraying or atmospheric plasma spraying [5]. Even if the anode substrate is made of the anode material, Ni/8YSZ, it has been found beneficial for the electrochemical performance to apply an additional anode layer which has a finer microstructure thereby ensuring better electrocatalytic conversion of the fuel gas [10]. The layers typically have thicknesses of 5–20 µm for the anode, 10–20 µm for the electrolyte and 50–80 µm for the cathode (Fig. 1). Nowadays the cathode also is composed of two layers: an electrochemically fine-grained composite of the electrolyte material and the electrocatalyst (lanthanum manganite), and a coarse current collection layer supplying air and electrons to the composite layer.

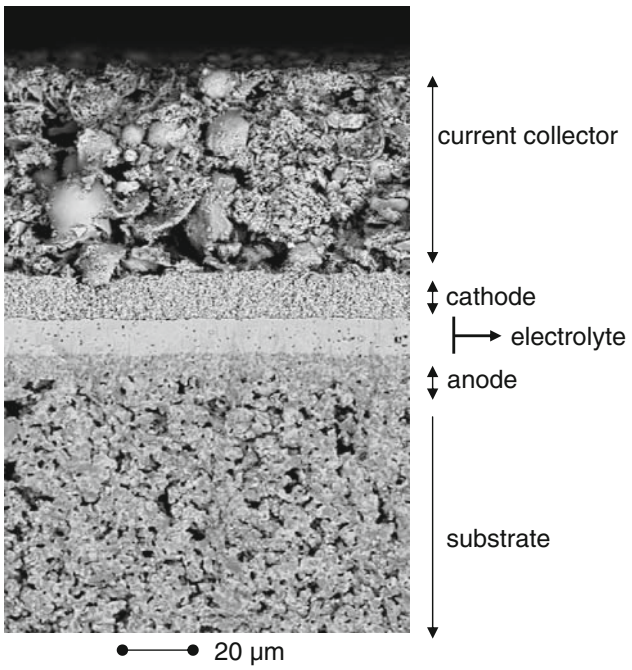

Fig. 1 SEM cross section micrograph of a typical 5 layer anode-supported SOFC manufactured at Forschungszentrum Jülich. It shows part of the 1.5 mm thick anode support layer of Ni-YSZ cermet, the 7 µm thick anode, the 10 µm thick electrolyte, the 15 µm thick cathode, and the 60 µm thick current collector layer

During the last 10 years, there have been three main areas of research for making SOFC technology competitive with other electricity generators:

1. *Cost reduction*: Several approaches have been undertaken to reduce the costs of materials, components, cells and stacks, e.g. by applying low-cost technical grade raw materials [2, 11, 12], by reducing the manufacturing costs (e.g. reduction of sintering temperatures, reduction of sintering steps [13], application of conventional ceramic or metallurgical processing methods, simplification of production processes etc.), by decreasing the thickness of components, especially the anode substrate, by integration of cheaper interconnect materials.
2. Higher performance, power density and efficiency have been targeted to lower the operating temperature. Simultaneously, this implies the aim of reducing degradation processes and costs (due to a smaller number of cells required for a certain gross power). Hence, higher performance gives more flexibility in operation and that is why the switch from electrolyte to anode-supported designs has taken place. Performance has been further increased by using new cathode materials and optimising their microstructure.
3. Another aspect related to costs is the aim of decreasing degradation processes and increasing durability and reliability (in operation and in component fabrication).

In the latter cases, it has been realised that this aim is easier to achieve with small-scale applications in the 1–5 kW class than with larger systems (100–1000 kW). Several degradation phenomena such as chromium poisoning of the cathode, contact resistances at the interfaces—especially at the interconnect—the long-term stability of electrolytes, anodes and cathodes, and the influence of fuel gases and contaminants (e.g. coking, sulphur poisoning) have been addressed. Several review articles have been published recently [14–16] and, due to the vast diversity of degradation phenomena, this topic will not be covered in this article.

This article is divided into three sections: The first deals with the materials used for the cell (electrolyte, electrodes) and the adjacent stack components (interconnects, coatings and sealants). The second section describes the manufacturing technologies for the various cell designs, and the third section deals with the microstructure of the electrochemically active layers of the cell, which is correlated with its power characteristics to illustrate the microstructure–property relationship in an SOFC.

SOFC materials

Electrolytes

An SOFC uses a solid oxide ion conductor as the electrolyte material. This material must have sufficient ionic conductivity for O^{2-} ions at operating temperature. In accordance with the aim of lowering operating temperatures, nowadays thin electrolyte films on porous electrode substrates are preferred. The four main material systems for the electrolyte are partially cation-substituted ZrO_2, CeO_2 and $LaGaO_3$ as well as apatites. The ionic conductivities of these solid electrolytes are listed in Table 1.

Apart from the apatite $La_{10}Si_6O_{27}$, the other solid electrolytes have an ionic conductivity which is about twice as high as that of 8YSZ at 800 °C as well as at lower temperatures. Therefore, although the improvement may be significant for electrolyte-supported cells, it is negligible for electrode-supported cells. Assuming an electrolyte thickness of 10 μm and an ionic conductivity of 0.05 and 0.12 S/cm for 8YSZ and 10 mol% scandia-stabilised zirconia (10ScSZ), respectively, at 800 °C (Table 1), this leads to an ohmic loss across the electrolyte layer of about 20 and 8 mΩ cm^2, respectively. These values are much smaller than the overpotentials at the cathode, which are in the range of 100–400 mΩ cm^2.

Only apatite, an ion conductor with excess oxygen ions on interstitial sites instead of oxygen vacancies as in the other materials, has a different temperature dependence and a smaller activation energy of the ionic conductivity. Therefore the value at 800 °C is rather low, but the material exceeds the conductivity of 8YSZ at 600 °C and also outperforms the other materials at ≤500 °C [17].

During exposure at 1000 °C, it was found that 8YSZ samples showed a higher decrease of conductivity than samples with a higher Y_2O_3 content [18, 19]. The best conductivity values after annealing were reached by samples with 10 mol% Y_2O_3. The ageing of zirconia stabilised with 7.8 mol% Sc_2O_3 directly correlated with the decrease in conductivity and temperature (700–1000 °C) [20]. Similar investigations with Sc_2O_3 contents between 8 and 12 mol% showed only slight degradation effects after ageing at 1000 °C for up to 6000 h. Samples with 11 mol% Sc_2O_3 remained nearly unchanged with respect to conductivity [21, 22]. Until now, however, the lower price and wider availability of yttria means that it is much more frequently used as a stabiliser in contrast to scandia.

The high ionic conductivity of the gadolinia-substituted ceria is superimposed by a p-type electronic conduction above 600 °C [23]. The electronic conductivity significantly increases at low oxygen partial pressures, which is attributable to a reduction of Ce^{4+} to Ce^{3+}. However, the problem with ceria is, above all, the poor sintering properties of the commercially available powders, which necessitates high sintering temperatures and causes interactions between CeO_2 and the YSZ layer [24, 25] when it is used as a diffusion barrier layer (see "Cathode" section).

Lanthanum gallate ($LaGaO_3$) is a poor ionic conductor. By replacing La^{3+} and Ga^{3+} ions with Sr^{2+} and Mg^{2+} ions, respectively, high ionic conduction is obtained [26]. Time-dependent measurements on $La_{0.8}Sr_{0.2}Ga_{0.85}Mg_{0.15}O_{2.825}$ [27] have shown that the conductivity at 700 °C in air is nearly unchanged and amounts to 0.073 S/cm over a period of 200 h. However, lanthanum gallate reacts with the NiO of the anode into a lanthanum-nickel oxide. This leads to a deterioration of the ionic conduction and the anode function. It was possible to suppress this reaction after applying an $(Ce,Sm)O_{2-x}$ interlayer, but the fabricated cell failed after 2000 h of operation [28].

Besides apatites, other oxide systems such as oxycuspidines ($RE_4M^{III}_{2-x}M^{IV}_xO_{9+x/2}$ or $RE_{4-x}M^{II}_xM^{III}_2O_{9-x/2}$) [29–32], mayenite ($Ca_{12}Al_{14}O_{33}$) [33, 34], gallates or $RE_{3-x}M^{II}_xGaO_{6-x/2}$ [35] or germanates $RE_{2-x}M^{II}_xGeO_{5-x/2}$ [36] (RE = rare earth; M^{II} = Ca, Sr; M^{III} = Al, Ga; M^{IV} = Ge, Ti) have been investigated in recent years. However, either due to the expensive raw materials (e.g. Ga_2O_3) or insufficient ionic conductivity, these materials are not expected to play an important role in the SOFC development.

Anode substrates and anodes

The most commonly applied anode material is a nickel/YSZ cermet [37]; a mixture of nickel oxide and YSZ powder is used as the starting material. In the final structure of the electrode, the nickel oxide is then commonly reduced to nickel during the start-up phase of the cell or stack by the prevailing fuel atmosphere. The nickel serves as a catalyst for the oxidation reaction of the hydrogen and is finely dispersed around the YSZ particles. The function of the zirconia skeleton is to stabilise a porous electrode structure, to create an extended reaction zone by increasing the amount of three-phase boundaries and also to match the thermal expansion coefficient between the nickel and the other cell components.

The demands made on the anode substrate such as good electrical conductivity, good gas permeability and fine-grained homogeneous microstructure can be realised by the powders currently used and were studied in detail for Ni/8YSZ anode substrates. At the stage of development where these demands on the component can be fulfilled reproducibly, consideration can also be given to technical powder qualities for cost reduction. Since the anode substrate accounts for more than 90% of the ceramic material expenditure of the ceramic parts, this component is the most promising candidate for material savings. Therefore, low-cost nickel oxides of technical powder quality were sought [11] to replace the NiO used hitherto, which satisfy very high demands on quality.

Because of the introduction of an additional anode functional layer (see Fig. 1), it is possible to divide up the two tasks of the Ni/8YSZ anode substrate, i.e. the mechanical stability and the electrocatalytic conversion of the fuel. This allows us to separately tailor the material properties of the anode functional layer and the anode substrate. Therefore, new cermets based on Ni/Al_2O_3 or Ni/TiO_2 were synthesised [38, 39] to match the thermal expansion coefficient of the 8YSZ thus avoiding thermo-elastic bending during cell fabrication [40] and reducing the costs of the substrate. However, during cell fabrication, a severe interaction with the anode layer was observed due to liquid phase sintering which led to a detrimental decrease of electrochemical performance.

Apart from cermets other materials can also be used as anode substrates, e. g. metals (ferritic steels) or ceramics with *n*-type conductivity. On the one hand, these alternatives offer solutions for the very important re-oxidation stability of anode cermets [41], because they do not undergo a strong volume expansion during re-oxidation. On the other hand, disadvantages like corrosion and chromium diffusion from the steel into the anode need further improvement. Also cell manufacturing is difficult because steels have to be protected from severe corrosion and highly conductive ceramics may lose their high electrical conductivity during sintering in air [42]. Therefore, either the electrolyte has to be deposited by plasma spraying [43, 44] or has to be sintered in an atmosphere of low oxygen partial pressure [45]. Furthermore, the cathode has to be applied without an additional sintering step [44].

Besides mechanical damage during re-oxidation, anode cermets also suffer from sulphur poisoning or coking from the fuel gas if the methane contains contaminants or insufficient amounts of water for internal reforming. Although efficient and compact de-sulphurisers are available and controlled system operation can solve these problems, there is an ongoing search for ceramic anode materials to overcome these drawbacks. In most cases, perovskite materials, such as $(Sr,La)TiO_3$, $(Sr,Y)TiO_3$, $(La,Sr)(Cr,Mn)O_3$, $(La,Sr)CrO_3$, $(La,Sr)(Al,Mn)O_3$, $(La,Sr)(Ti,Mn)O_3$, have been investigated for this purpose [46]. With pure ceramics, however, cell performance has always been significantly lower than for the conventional Ni/8YSZ anode, because these anodes either do not have sufficient electronic or ionic conductivity or are not catalytically active. Actually, there are approaches to improve performance using ceramic composites with small additions of catalysts [47–49] and the cell performances or anode overvoltages achieved show very encouraging data when composites of an ion conductor, an electronic conductor and a catalyst are applied, e.g. $(Sr,Y)TiO_3$/YSZ/Ru [48], $(Sr,Y)TiO_3$/YSZ/Ni [49], $(Sr,La)TiO_3$/YSZ/Pd–CeO_2 [50]. An interesting approach is the use of $(Sr,La)TiO_3$ as the anode substrate and a thick anode layer of Ni/YSZ taking advantage of the high conductivity in reducing atmosphere and the redox stability of $(Sr,La)TiO_3$ combined with the superior electrocatalytic properties of Ni/YSZ cermets [51]. Such button cells delivered about 1 A/cm^2 at 0.7 V and 800 °C, and also demonstrated improved sulphur tolerance and stability with respect to coking in natural gas. The first anode-supported half-cells manufactured with dimensions of 5×5 cm^2 using $(Sr,Y)TiO_3$/YSZ as the anode substrate and YSZ as the electrolyte showed no significant increase of gas leakage across the electrolyte after numerous redox cycles between fuel gas and air, thus demonstrating the feasibility of larger cells with reliable mechanical integrity of the electrolyte layer [52].

A wider range of anode materials—also including more exotic possibilities—are described in recently published articles [46, 53–57].

Cathode

Perovskite materials of the ABO_3 type are generally used as the cathode material. A frequently used material is lanthanum manganite ($LaMnO_3$) with substitutions of

strontium or calcium at the A-site [58, 59]. Both A- and B-site substitutions have been investigated extensively so that these ceramics can be selected according to the demands made on their properties such as thermal expansion coefficient, electronic or ionic conductivity and chemical interaction with the electrolyte.

Lanthanum or strontium cobaltites have attracted much attention because of their high mixed ionic-electronic conduction [60]. Indeed, (La,Sr)CoO_3 shows a higher cathodic performance than (La,Sr)MnO_3, but the cobaltite possesses a very different thermal expansion in comparison to YSZ [61] and it reacts readily with this electrolyte at high temperatures (≥800 °C) forming highly resistive $La_2Zr_2O_7$ or $SrZrO_3$ compounds. These unfavourable solid-state reactions can be avoided if a ceria-based diffusion barrier layer is applied [62]. As a compromise between thermal expansion mismatch and electrochemical performance, the composition $La_{0.6}Sr_{0.4}Fe_{0.8}Co_{0.2}O_3$ (LSFC) has been established as an alternative to (La,Sr)MnO_3 cathodes for reduced operating temperatures since the mid 1990 s [62, 63]. SOFCs with cathodes of similar LSFC composition reach current densities of 1.5–2 and about 1 A/cm^2 at 800 and 600 °C, respectively, and at 0.7 V [64].

The advantage of such mixed ionic–electronic conducting cathodes is their increased reactive catalytic surface area over the whole perovskite grain. Therefore, the charge transfer of adsorbed oxygen atoms takes place directly on the perovskite surface [65]. The increase in oxygen ion conductivity and hence in mixed conductivity is generally correlated with an increasing thermal expansion [66]. Therefore, an improvement of the transport properties is always linked to an increasing mismatch in thermal expansion relative to the other cell components.

A rough classification of cathode materials regarding their electrocatalytic activity follows the order: $LaCoO_3 > LaMnO_3 > LaFeO_3 > LaCrO_3$ [67]. The electrocatalytic activity also varies with alkaline-earth concentration in the perovskite. In general, the electrical and ionic conductivity, the thermal expansion coefficient and the catalytic properties increase with increasing alkaline-earth content between $0 < x < 0.5$ in $La_{1-x}A_xBO_3$ with A = Ca, Sr, Ba and B = Cr, Fe, Mn, Co. The extreme case is $Ba_{1-x}Sr_xCo_{0.8}Fe_{0.2}O_{6-\delta}$, which shows extraordinarily high thermal expansion and high oxygen ion mobility [68, 69]. It is, therefore, not surprising that cells with this cathode material result in very high power output [70]. For practical applications, however, this material is not useful due to the large thermal expansion mismatch with the other cell components and the formation of barium carbonate in the presence of CO_2 in the oxidant gas leading to rapid and severe performance loss [71, 72].

For the past several years, more number of complex perovskites such as double perovskites ($A^{III}A^{II}B_2O_{5+\delta}$ typically with A^{III} = RE, A^{II} = Ba and B = Co) and $K_2NiF_{4+\delta}$-type materials have been under investigation. Compared with the ABO_3 perovskites, the double perovskites possess ordered oxygen vacancies in the $A^{III}O$ layer resulting in two different coordination spheres for the cobalt ions [73] and high oxygen ion mobility, [74, 75]. The first cathode tests, however, do not show significant differences to cobaltites of similar composition (e.g. $RE_{0.5}Sr_{0.5}CoO_{3-\delta}$) [76], and it is also likely that these Ba-containing cathode materials are prone to reactions with CO_2.

Materials with $K_2NiF_{4+\delta}$-type structure like $A^{III}_{2-x}A^{II}_xBO_{4+\delta}$ with A^{III} = RE, A^{II} = Ca, Sr, Ba and B = Mn, Fe, Co, Ni, Cu typically have lower electronic conductivity than the analogous ABO_3 perovskites [77, 78], but the ionic conductivity and oxygen exchange kinetics can be very high due to excess oxygen ions on interstitial sites [79–81]. It is worth noting that the activation energy of ionic diffusion is significantly smaller than for cathodes with oxygen vacancies. Hence, the cathode polarisation is low [82], and SOFCs with nickelates as cathodes have shown very promising current densities of about 1.2 and 0.6 A/cm^2 at 800 and 600 °C, respectively, and 0.7 V [83, 84] making them interesting cathode materials especially at reduced operating temperatures.

Interconnect

The interconnect in SOFC stacks is the component which electrically connects the single cells and in planar systems additionally separates the gas compartments from each other. In an SOFC system, numerous demands are made on the interconnect, such as good electrical conductivity, gas tightness, chemical compatibility with the adjacent components of the fuel cell, high corrosion resistance to the reaction gases, matched thermal expansion and, last but not least, reasonable costs. In order to meet all these requirements, two classes of materials are commonly used for interconnects, namely ceramic and metallic materials [85]. Whereas ceramic interconnects played a dominant role in early SOFC developments, metallic interconnects have also been frequently used in recent developments and are the favoured materials worldwide today due to the general trend towards lower operating temperatures.

Practically all ceramic interconnects are based on $LaCrO_3$-type materials because this is one of very few perovskites that do not decompose in the fuel gas atmosphere. However, due to the electrical conductivity required, lanthanum chromites cannot be used at temperatures lower than 800 °C. In addition, lanthanum chromites show undesirable swelling in reducing atmospheres caused by the reduction of Cr^{4+} ions to Cr^{3+} and the formation of oxygen vacancies [86] leading to strong internal stresses and possible cracking during operation.

Apart from these physical handicaps, costs are high for the $LaCrO_3$ and for the processing of the layers. Hence, the advantages of metallic interconnects are obvious: high electrical conductivity, good ability for processing and lower costs. The disadvantages, however, are corrosion in combination with increasing resistance during operation, chromium evaporation and unsatisfactory high-temperature strength.

The long-term stability of the metallic interconnect is essentially governed by the corrosion characteristics. The materials used for interconnects are alloys which form chromium oxide, thus ensuring sufficiently high conductivity for thin oxide scales. Meanwhile, several ferritic steels have been developed especially for SOFC application containing only very small amounts of aluminium and silicon to avoid the formation of highly resistive oxide scales and low amounts of manganese for the formation of $(Cr,Mn)_3O_4$ spinels as the outer corrosion scale [87–89].

The main focus in interconnect development is still the improvement of corrosion behaviour, but also the reduction of the contact resistance of the oxide scales or in combination with coatings and the reduction of chromium evaporation to avoid a detrimental poisoning of the cathode with chromium species [90–96]. All these phenomena make a major contribution to the observed degradation of stack voltage during operation, although it is not yet clarified to what extent.

Protective and contact coatings

Many attempts have been made to reduce the damaging effect of chromium vapours on the cathode side by suitable protective layers. The first approach was plasma-sprayed coatings of lanthanum chromite as a protective method to minimise the evaporation of volatile Cr species [97, 98]. The function of these coatings as diffusion barriers against volatile Cr species strongly depends on the quality of the layers (gas tightness, crack density) and may not always be as effective as expected. In addition, for anode-supported cells, the plasma-sprayed chromite coatings are characterised by high contact resistances and high fabrication costs in comparison to ceramic methods using slurries or pastes. However, the reactivity of lanthanum chromite with metals, either with Cr- or Fe-based alloys, is low and the metal/ceramic interface is very stable under operating conditions.

Chemical interactions between coatings and interconnect material increase when the alkaline earth content in the ceramic is increased. Often perovskite materials have been brought in contact with Cr-based alloys or steels and the formation of chromates (e.g. $CaCrO_4$ or $SrCrO_4$) was observed [97, 99–101] leading to the progressive decomposition of the perovskite material and a brittle interface. As a consequence of these interactions, the application of cobalt oxide or cobalt manganese spinel between the perovskite and alloy was investigated [100, 102–105] and showed stable contact resistance over time.

Coating the ferritic steel Crofer22APU by wet powder spraying with a porous Co_3O_4 layer or a metallic Co layer leads to the formation of a new dense Cr-free reactive layer under SOFC operating conditions [102]. As a reaction product of Mn from the oxide scale of the steel and the Co_3O_4 layer, this dense layer may act as a barrier against the vapour phase transport of volatile Cr species.

Contact materials are electrically conductive ceramics applied to improve the contact between interconnect and electrode. Whereas for the anode side metallic materials are used (as mesh, foam or paste), the cathode side is often coated with ceramic cathode-like compositions having conductivities in the range of 50–500 S/cm. Because there are no electrochemical requirements to be obeyed for the contact materials, they can vary significantly from the electrode materials and be optimised with regard to other physical and chemical properties than the electrodes. Apart from the electrical conductivity, the most important properties are the thermal expansion and sintering behaviour at assembling temperatures in the range of 800–1100 °C. Because the contact layer thickness may vary between 30 and 200 μm and ceramic materials heat treated below 1000 °C are usually very porous, the specific conductivity of the material should be high. This is, in fact, the case for lanthanum cobaltites which have specific conductivities up to 1700 S/cm [106]. In contrast, the thermal expansion of these cobaltites has a strong mismatch with the other cell components. For electrically conductive ceramics, therefore, a compromise between acceptable conductivity and tolerable mismatch in thermal expansion has to be made as for the cathode materials.

Sealings

In planar SOFCs, gastight seals must be applied along the edges of each cell, along the outer edges of the stacking layers and the gas manifold to separate the two gas compartments and to insulate the stacking layers from each other.

Glass or glass ceramics are frequently applied for joining metals, especially the joining of steels [107]. Many of these products are available commercially, but most of the sealing products are produced for low-temperature joining and for room temperature applications. However, no commercial product fulfils the requirements of a thermal expansion coefficient in the range of $10–13 \times 10^{-6}\ K^{-1}$ up to high temperatures. Therefore, many SOFC developers started their own sealing development.

Most studies have been carried out on barium calcium alumino-silicate (BCAS) and barium calcium magnesium

alumino-silicate (BCMAS). The comparison of BAS, CAS and MAS glasses using B_2O_3 as a fluxing agent and TiO_2, ZrO_2, NiO and Cr_2O_3 as a nucleating agent showed that the barium glass tended to react with chromium steel more than the other glasses, displayed faster crystallisation and appropriate thermal expansion [108, 109].

BCAS glasses and ferritic steels easily form $BaCrO_4$ in the presence of oxygen [110]. Studies by Yang et al. also clearly showed that the sealing material alone does not lead to good joining. It is more important to adapt the interconnect/sealant couple.

Under oxidizing conditions, the formed oxide scales of ferritic steels (chromium oxide scale at the inner interface to the steel followed by a scale of manganese chromium spinel at the outer interface towards the glass) are partially dissolved by the glass. This leads, on the one hand, to good adhesion and mechanical sticking between sealant and steel, and, on the other hand, however, to a destabilisation of the steel at the three-phase boundary glass/metal/air [111, 112]. Thus, good adhesion and stability against corrosion may become conflicting objectives.

Besides glass–ceramics, compressive seals and brazing systems have also been investigated [113]. In the case of compressive seals, metallic gaskets and mica-based materials (vermiculite, phlogopite) were tested. None of the seals is hermetically gastight and require high mechanical loads to achieve low leakage rates [114, 115]. To the best of our knowledge, no stack has yet been successfully operated with such sealing systems. Also, the brazing has not yet reached a reliable applied status. However, the use of Ag–CuO–Ti brazes in combination with an insulating layer seems to offer technologically interesting alternatives to glass–ceramic sealants [116, 117]. The application of brazes on thin interconnect components has shown that (a) the interaction at the braze/ferritic steel interface is strongly dependent on the steel pre-treatment [117, 118] and (b) mechanical failure is observed at rather low mechanical load [118]. Brazing on untreated steels revealed a reaction zone of oxides containing Fe, Cr and Cu with large amounts of Fe, thus indicating that no protective chromia scale could be formed during brazing. In the case of pre-oxidised steel samples, the oxide scales consisted of Cr and Cu oxides. The observed crack formation always took place within the brittle reaction zone [118].

SOFC manufacturing technologies

The fabrication processes for SOFCs can be distinguished in different ways. The following should be mentioned:

- Geometrical design: e.g. planar, tubular or hybrid forms
- Mechanical support: e.g. anode-, electrolyte-, cathode-, metallic- or inert-supported
- By processing technologies, e.g. ceramic (wet chemical technology plus thermal treatment), thermal (e.g. plasma or flame spraying) or gas phase deposition techniques
- By thickness of the component/layer, e.g. thick (>100 μm), thin (5–100 μm) and ultra-thin (<5 μm)
- Or by substrate and functional coatings

For this presentation, the manufacturing technologies are divided according to the group of technologies. That means the techniques are described in the following order: firstly, ceramic processing methods, secondly, thermal spraying methods, and, thirdly, physical, chemical and electrochemical technologies. In particular, the chapter on ceramic processing methods is subdivided into substrate and coating technologies. All the substrate manufacturing and coating technologies are not only described technologically but also with respect to industrialisability. That is to say, the current status of the technology is discussed with respect to its industry level (laboratory scale, technological scale, industrial scale, complete continuous production line).

Ceramic processing methods

Substrate

Tape casting (TC) The tape casting technique is widely used in the ceramics industry to manufacture two-dimensional thin dense or porous supports. Thicknesses range from approximately 100 to 800 μm in the final fired state. For SOFCs, TC is used mostly for fabrication of the mechanical bearing support for planar designs. For electrolyte-supported cells, usually a 100–200 μm thick 8YSZ tape is cast and sintered to full density. For electrode-supported cells, the electrode is cast typically in thicknesses of 250–500 μm, and the support needs to be porous to ensure gas diffusion.

Typical slip formulations can be found in [119–123]. As an example, the slip of an anode support developed at Forschungszentrum Jülich is described in more detail. The anode support consists of nickel oxide and 8YSZ in variable ratios, typically 50:50 wt%. The powders are suspended in an azeotropic mixture of solvents, e.g. methylethylketone (MEK) and ethanol (EtOH), in a ratio of 2:1 wt%. As organic additives, binder(s), dispersant(s), plasticiser(s), de-airers, surfactants and wettability optimisers are added. The necessary porosity in the final electrode is either ensured by the organic additives added; or, if a higher pore volume fraction is to be obtained, then pore formers, such as polymers, rice starch or graphite, are also added. The slip consisting of powder, solvents and organics must be outgassed before casting. The casting

itself [119] is done by transporting the slip into a reservoir, which is open on the bottom side. Under the reservoir, a polymeric tape is transported, and the slip covers the transport tape. The transport tape and the coated slip are moved through one or two blades ('doctor blades'), which ensure slip thickness and uniformity over the width of the tape. Subsequently, the tape is moved into a well-controlled drying chamber. After drying, the tape formed can be cut by, for example, knife cutting or punching into the envisaged geometries. After cutting, the substrates can either be pre-sintered to de-binder the material and to form a substrate that is easy to handle for the subsequent functional layer coatings, or the 'green' (non-sintered) tape can be coated directly with, for instance, anode and electrolyte and afterwards co-fired with the substrate. In both cases, the firing temperature of the electrolyte to gas-tightness is below the highest temperature within the complete manufacturing process (typically 1400 °C). The electrolyte supports are always sintered to gas-tightness before coating with the functional layers. For almost all anode-supported cells and for all electrolyte-supported cells, the substrate is now manufactured by tape casting [124–130]. The geometries which can be fabricated range from 50 × 50 mm^2 for single cells (or 50 mm in diameter) up to 200 × 400 mm^2 for cells for power stacks.

In recent years, efforts have also been made to cast metals to form metal-supported SOFCs [131]. Here, typical SOFC interconnect materials like Crofer22APU [132], ITM [133] or others were cast in the same way as described above. The basic differences are the casting thicknesses and the slip formulations. Normally, oxide powders have a smaller particle size distribution (1–10 μm) than metallic powders (<45 μm for these applications), and, thus, the slips for metal powders must be more viscous to avoid separation or unwanted graded structures. In addition, the sintering conditions (vacuum or inert gases, T_{max}) and the coating technologies for the metal supports (mostly thermal spraying) differ from those for ceramic supports.

Pressing methods Another technology for forming two-dimensional thin substrates is the pressing of powders by cold, warm, hot, cold-isostatic (CIP) or hot-isostatic pressing (HIP). The main disadvantage of the pressing techniques in comparison to, for example, tape casting is that they operate discontinuously, i.e. each process of filling, optionally heating up, pressing, and demoulding is done unit-by-unit. This is time-consuming and is thus now used less frequently for SOFC substrate manufacturing. In the ceramics industry, these methods are mostly used for smaller geometries with complex structures. Especially the techniques, CIP and HIP, are only applied for extremely dense three-dimensional structures because they need complex machines. Therefore, for SOFC manufacturing only cold and warm pressing are used in certain cases. Pressing techniques are applied in particular if thicker substrates need to be manufactured (thickness >800 μm). The reason is that, for example, tape casting requires too much time for the drying of such thick tapes. One example of the use of a pressing method for SOFC substrates is the manufacturing of thick (1 or 1.5 mm) anode supports for large cells for power stacks [134, 135]. Here, a pre-conditioned powder mixture known as Coat-Mix® powder is used. A special technique is used to mix the substrate materials (NiO and 8YSZ) together with a polymeric resin. By adding water to the acid solution, the solubility of the resin is reduced and it subsequently precipitates at the powder surface and, after a drying step, a flowable powder mixture is formed. This powder is then filled into the pressing unit and pressed at moderate pressure (~1 MPa) at approximately 100 °C to two-dimensional substrates with dimensions of to 350 × 350 mm^2. After de-bindering and a pre-sintering step, the porous substrate is coated with the functional layers according to the scheme described in the "Tape casting" section.

Extrusion Extrusion is used in the ceramics industry if a continuous structure with an elongation in one direction is necessary. Typical geometries are tubes, rectangles, triangles and derived structures with or without inner structuring (e.g. clay bricks).

For SOFCs, this technique is mostly used for the Siemens tubular cathode support [136] and the Rolls-Royce flat tubular inert-supported design [9]. Its use for planar designs is limited because the ratio between substrate width and substrate thickness is limited. If the envisaged width is, for instance 100–150 mm, then the substrate thickness is roughly >2 mm. The technique consumes a great deal of material because sizes of the same shape can be manufactured by tape casting in thinner structures. However, for the tubular and quasi-tubular designs, extrusion is the appropriate technique.

For extrusion, the powders are usually mixed with water-based plastics. Owing to the time-consuming drying step, the amount of water should be as small as possible; thus, in most cases, water-soluble binders are added (e.g. methylcellulose, polyacrylamide, polyvinyl alcohol etc.) to minimise the water content. The major difference between extrusion and tape-casting slips is the viscosity. Extrusion slips have extremely high viscosities in the range of 1000 Pa s while tape-casting slips are in the range of only some Pa s. After extrusion, the tube is cut into the desired length by wire-cutting. For SOFC fabrication, the substrate is usually de-bindered and sintered before coating with functional layers. The sintering of both the cathode and the inert support is performed at high temperatures (>1400 °C), which ensures no dimensional changes of the

support and, therefore, uniform structures for the subsequent coating and sintering steps.

Calendering Calendering means the connection of more than one thin planar structure by pressing them together during rolling between two or more rollers. The technique is continuous and is used to combine the substrate with one or two functional layers pre-fabricated by, for instance, tape casting. Hence, calendering is a technique performed between substrate manufacturing and coating. Normally, it is limited to tapes of relatively similar thicknesses, which means that it cannot be used to combine, for example, a thick substrate (1.5 mm) with a very thin anode and electrolyte (<10 μm). It can, however, be used to combine thin supports (<500 μm) with relatively thick functional layers >20 μm. Owing to the rolling-pressing of the different tapes in the 'green' state, they are 'glued' together by the remaining organics. A prerequisite for calendering is, therefore, the use of similar organics for all tapes or the use of organics which do not interact during calendering, de-binding, and sintering. In SOFC calendering as used by AlliedSignal [137,] normally half-cells consisting of the support, one electrode and the electrolyte are produced. A subsequent coating step with the second electrode is added after the first sintering. Table 2 lists the substrate manufacturing techniques, the geometries to be fabricated with the respective technique and some slip/paste/suspension information.

Summary of substrate manufacturing techniques As SOFCs move closer and closer to the market, substrate manufacturing techniques which are continuous and which are already established in other application fields have been used. The trend is clearly moving to extrusion for tubular designs and to tape casting for planar designs. Discontinuous or time-consuming technologies are increasingly ruled out. In addition, there is an obvious tendency towards thinner supports to minimise materials costs. For example, 10 years ago, anode-supported cells were normally 1 mm thick, whereas nowadays they are 300 mm or less. The same trend is observable for electrolyte-supported SOFCs (from 250-μm support thickness down to ~100 μm). Another direction is to form the necessary porous microstructure 'intrinsically', which means not by adding special pore formers but only the organics used for fabrication. If pore formers are necessary, then there is a shift towards using cheaper ones (e.g. rice starch) rather than special polymers or graphite.

Coatings

Various technologies can be applied for coating SOFC substrates. At least three different groups can be mentioned:

- wet chemical or ceramic technologies like SP slip casting or spraying methods
- thermal spraying technologies like atmospheric or vacuum plasma spraying, and
- gas phase deposition techniques like chemical (CVD), electrochemical (EVD) or physical vapour deposition (PVD)

Nearly all the technologies from the three groups have been applied. There are numerous reasons for using one particular coating technology for a special layer. For instance:

- *layer thickness*: thermal spraying normally leads to layers with thicknesses of more than 30 μm, ceramic technologies lead to coating thicknesses ranging from typically 5 to 100 μm, and the third group is applied for thin films (less than ≈2 μm)
- *layer microstructure*: thin and dense layers can be obtained by CVD, EVD and PVD; ceramic coating

Table 2 SOFC substrate manufacturing technologies and typical characteristics

Substrate manufacturing technique	Geometries	Substrate characteristics (in final fired state)		Slip/paste/suspension characteristics
		Thickness	Elongation	
Tape casting	Planar	100–800 μm	20 × 20 to 400 × 400 mm^2	Low viscosity (Pa s); azeotropic solvents, various organics
Pressing	Planar, microtubular (CIP, HIP)	Planar 500–2000 μm; microtubular wall thickness 100–500 μm	Planar 20 × 20 to 400 × 400 mm^2; microtubular tube length up to 100 mm, ∅ up to 10 mm	High viscosity or simple powder mixture; pressing agent, fewer organics
Extrusion	Planar, tubular, quasitubular	Wall thickness 500–2000 μm	Planar 100 × 400 mm^2[a]; tubular ∅ up to 10th cm, length up to m	High viscosity (1000 Pa s), water-soluble binders, additional organics
Calendering	Planar	100–2000 μm	Comparable to tape casting (TC), depending on TC single tape size	As TC basics

[a] More important than the effective size is the ratio width/length

technologies can be used either for dense or for porous layers, and plasma spraying normally leads to less porous layers with or without segmentation cracks
- *substrate type*: for ceramic substrates, typically also ceramic coating technologies are applied; for metal substrates thermal spraying techniques are used in most cases because if oxide layers applied by wet chemical technologies are coated, then they must be sintered in air, and the metal will oxidise, forming either insulating oxide scales or involving the risk of corrosion or scale spallation
- *substrate geometry*: tubular designs cannot be coated by technologies like SP because this is a two-dimensional coating technique; vice versa a dip process can easily be applied to tubular geometry by dipping the porous support into a tank with the coating suspension. If fine structures need to be obtained, e.g. for the Rolls-Royce quasi tubular design, then this rules out technologies which have been developed for large sizes (e.g. plasma spraying)
- *costs*: all manufacturing steps including materials and processes must be able to be integrated into an industrial production line to reduce fabrication costs

In the following, the most frequently applied coating technologies for state-of-the-art SOFCs and some new manufacturing technologies are presented.

Screen printing (SP) The most widely used coating technology for ceramic planar supports (electrolyte, anode or cathode) is SP In the case of electrolyte-supported SOFCs, both electrode layers are coated by SP, and for the anode- or cathode-supported designs, the functional electrodes and the electrolyte are applied by SP.

For SP typically pastes consisting of the powder, a binder, e.g. ethyl- or methylcellulose, and a solvent, e.g. terpineol, are used. Typical amounts of powder are in the range of 60%. Similar to tape-casting slips, the paste viscosities are also in the range of few Pa s. However, the rheological behaviour must have a special time dependence. This behaviour can be characterised by the SP process itself. The paste is pressed through a screen by a squeegee. While being pressed through the mesh, the paste must flow, and after removing the screen from the substrate to be coated, the paste must fill the remaining channels formed by the chaining and weft thread of the screen. After filling the cavities, the paste must stop flowing to ensure the dimensional accuracy of the layer. In most cases, the so-called pseudo-plastic rheological behaviour is preferred.

Screen-printed layers have, after sintering, thicknesses ranging from $\sim$5 to $\sim$100 μm depending on layer characteristics, screen used and z-direction shrinkage of the dried coating. Typically, the wet thickness is 3–4 times the dried thickness, and the dried thickness one and a half times to double the sintered thickness. Typical particle sizes for screen-printed layers vary from 1 to $\sim$15 μm. With SP, dense and porous layers can be obtained, thus either the electrolyte or the electrodes can be printed.

During manufacturing of electrolyte-supported cells, both electrodes can be printed and co-fired at temperatures between 1000 and 1200 °C, if the right particle size distributions and the right material ratios are used (LSM:8YSZ for the cathode and NiO:8YSZ for the anode). For anode-supported cells the sintering of the electrolyte and the second electrode is done separately. The reason is that for dense sintering of the electrolyte high temperatures are necessary ($\sim$1400 °C). By contrast, the cathode does not withstand such high temperatures. It either decomposes or it also densifies, thus drastically reducing the amount of three-phase boundaries and subsequently losing cell power, or it interacts with the electrolyte material forming insulating phases (e.g. lanthanum zirconate). The latter possibility, the interaction between the electrolyte material 8YSZ and high power density cathode materials, e.g. La–Sr–Fe–cobaltites, takes place at relatively low temperatures (<1000 °C). However, typical sintering temperatures for these LSFC cathodes are 1050–1100 °C. Thus, a barrier layer must be introduced inhibiting the diffusion of La or Sr to the 8YSZ. This barrier layer, typically ceria-gadolinia or ceria-samaria oxide, is also applied by SP and sintering.

SP is also used to coat the functional layers in the Rolls-Royce quasi tubular design. However, only the flattened broad sides of the inert support were coated and, thus, the technique can also be applied to geometries which are not exclusively planar. The rounded edges are not coated with the functional layers.

Typical current densities for anode-supported cells based on tape-cast substrate and screen-printed functional layers are in the range of 1.3–1.5 A/cm^2 if an LSM/YSZ cathode and an LSM current collector are used (single cell test at 800 °C and 0.7 V with hydrogen/water vapour and air, 50 × 50 mm^2 and 40 × 40 mm^2 active area).

The SP technique is industrially established, scalable, and can be introduced in a production line. Thus, it is ideal for low-cost fabrication with high throughput capacity [138].

Recently, efforts were made to use the SP technique to apply thin-film electrolyte layers by combing the solid part within the paste (the powder) with additional sols of the same composition (e.g. YSZ or CGO sol), which enables smaller particle sizes, and possibly lower sintering temperatures and thinner layers [138–146]. This development would be beneficial for reducing manufacturing costs (lower T_{Sint}) and reducing ohmic losses (thinner electrolyte) for SOFC use with classical materials, but at lower operation temperatures.

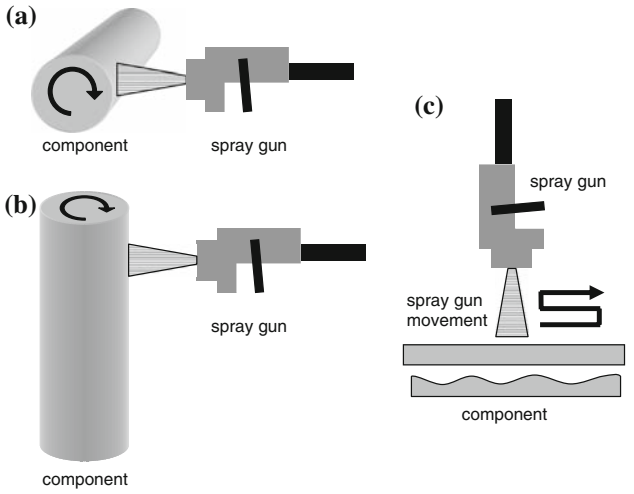

Fig. 2 Positions of spray gun and component to be coated; **a** horizontal/horizontal, **b** horizontal/vertical, both with tubular designs and **c** vertical/horizontal with planar and planar structured designs

Spraying methods The spraying of liquids for coating planar, tubular and three-dimensional structures is widely used in various industries, e.g. automobile, white goods (dishwashers, washing machines etc.), electronics. In many cases, this technique is used for large components aiming for thin homogeneous layers (e.g. paints). Spray techniques can work with horizontal parts, subsequently the spray stream moves vertically, or with vertical or horizontal parts (or even tubular parts by turning the tube) and a horizontal spray stream. In Fig. 2, this is illustrated schematically.

The main advantage of spraying techniques in comparison to, for example, SP is that by spraying, non-uniform and non-planar geometries can also be coated. This is illustrated in Fig. 2c. Planar structures were coated homogeneously by meandering the spray gun over the component. In all the cases, spraying techniques suffer from overspray. The formation of overspray has two disadvantages: the coating efficiency is reduced and, consequently, the costs are higher (even if the overspray is recycled, it must be re-cleaned, and a recycling system has to be installed) and by meandering over the parts, the meander steps must be very well adapted to suppress inhomogeneous coating thickness because of different overlapping courses.

If structured planar geometries are to be coated, then the rheological behaviour of the spray suspension must also be very well adapted. If the viscosity is too high, then the coating thickness differs between the top and the bottom parts due to insufficient flow (thicker on the hills, thinner in the valleys), and if it is too low, then the case is vice versa (thicker in the valleys and thinner on the hills). The coating homogeneity is, therefore, a combination of suspension rheology and adhesion of the suspension to the component to be coated.

For solid oxide fuel cells, spraying techniques like wet powder spraying (WPS) [147] can be applied twice. First, for the coating of the functional layers on the mechanical support irrespective of the support and the layer to be coated (e.g. electrolyte-, anode-, cathode- or inert-supported and all layers), and, secondly, for the coating of the metallic interconnects with protection or contact layers. Especially the interconnect coating is of interestbecause it typically contains channelled structures for the gas distribution. These channels can be rectangular in shape, of trapezoidal design or may have a wavy-like structure. Even rectangles with 90° edges can be coated, but due to the relation between the spray direction and the different coating directions (horizontal to the spray gun or parallel) the coating thickness, homogeneity and quality differ. Figure 3 shows as an example of two typical channel structures of metallic interconnects and some coatings.

From Fig. 3, it can be seen clearly that insufficient adhesion or spreading behaviour of the spray suspension leads to

- lens-like coatings on the hills (leading to minimised contact area between the cathode or current collector and the contact layer), especially for rectangular gas channels
- thick coatings in the gas channel edges or at the gas channel ground (leading to enhanced cracking during suspension drying)
- thin, uneven coatings on the channel walls (rectangular design)

Such complex structures with ‘hard’ edges and walls parallel to the spraying direction cannot be coated totally homogeneously. In the case of the metallic interconnect for SOFCs, the homogeneity is important but it need not be 100%. The necessary homogeneity depends on the special layer and its function within the stack. As an example, the chromium evaporation protection layer ensuring the formation of a special crystal that evaporates less volatile chromium species than the typical chromia layer needs to be coated at every free metal surface. However, the thickness is not the key factor, which means it can vary from e.g. 5 to 10 μm. On the other hand, the contact layer must have a minimum thickness to ensure safe and complete contacting of the whole cell to the interconnect, thus a minimum thickness needs to be maintained.

One application of the WPS technique to the SOFC itself is the coating of the cathode and the electrolyte on the older tubular Siemens design. Here the tubes or quasi-tubular geometries are coated with a vertical spray gun and by horizontally turning the tubes (Fig. 4).

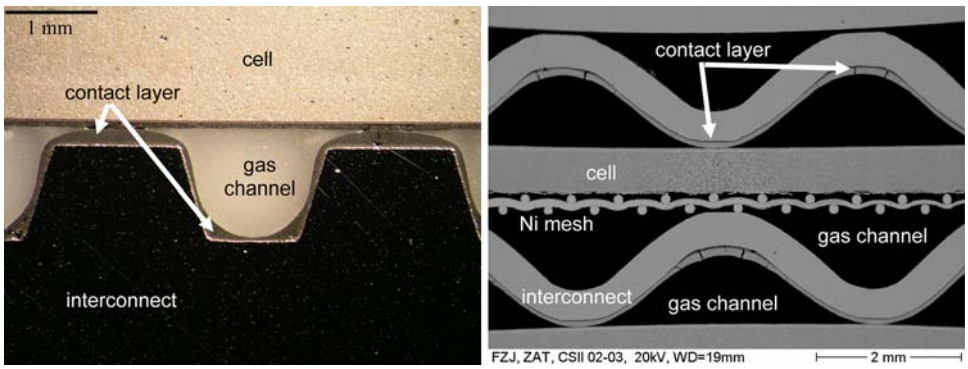

Fig. 3 WPS coating of contact layer on an interconnect with trapezoid gas channels (*left*) and sinusoidal channels (*right*)

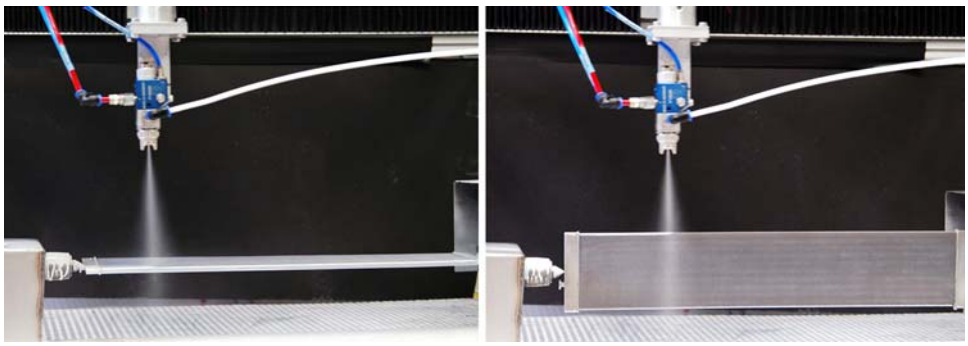

Fig. 4 Coating of tubular and quasi-tubular SOFCs with electrolyte (planar and edged part of a flat tube)

In principle, the technique may also be used to coat net or mesh structures with functional layers (e.g. Ni-mesh in SOFCs).

Nowadays, the technology is used for the cathode coating of ASCs at Topsøe Fuel Cells [124, 125] and for interconnect coating at Forschungszentrum Jülich [148].

Electrophoresis and electrostatic spraying Electrophoresis (EP) and electrostatic spraying (ES) have up to now only attracted limited attraction with respect to large-scale manufacturing of SOFCs. A few groups utilise both technologies on the laboratory scale [149–151]. The basics of EP can be found in [152, 153]. Only Ceres Power [154] manufactures the electrolyte on metal-supported SOFCs on a commercial scale. No other R&D has been scaled-up to realistic cell dimensions for SOFC stacks or used to manufacture increased amounts of cells. Therefore, no detailed description of these technologies is presented here.

Slip casting Slip casting and especially vacuum slip casting (VSC) is a coating technique for planar or tubular porous substrates. An open porosity is a prerequisite for film formation because during VSC a simple slurry, composed of the powder, ethanol and an organic binder, is applied on top of the planar substrate, or a tubular substrate is inserted into the slurry, from the back side of the planar substrate or inside the tube vacuum is drawn, the dispersant migrates through the porous support and a smooth and homogeneous powder layer is formed. The technology

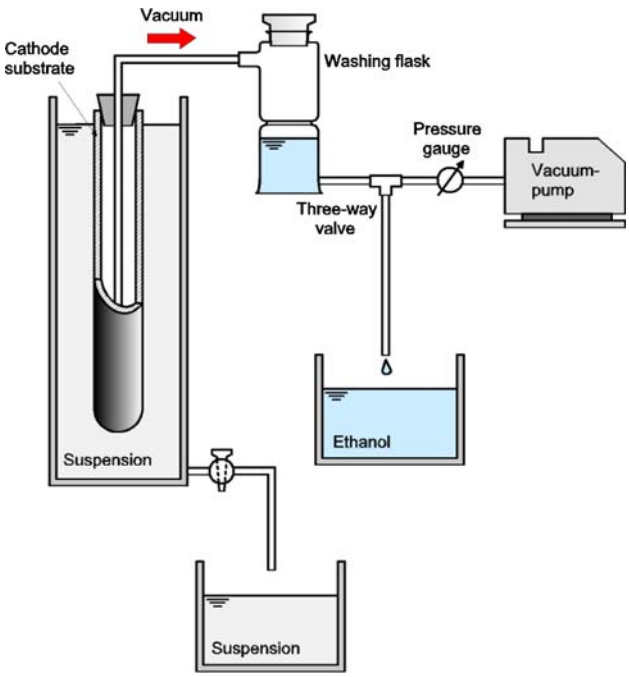

Fig. 5 Schematic of vacuum slip casting (tubular cathode substrate)

works like a filtration process. For SOFCs, the technique is mostly used to coat anode-supported cells with the anode and the electrolyte layer. Both the anode support and the anode itself are porous and thus both layers, i.e. the anode and the electrolyte, can be coated by this technology. The basic principle is shown in Fig. 5. By using sub-micron-sized

particle distributions (~100–500 nm), fewer requirements have to be met with respect to suspension stability, deflocculation, sedimentation etc. By doing so, very thin, even and extremely homogeneous layers of thicknesses from 1 to 20 μm can be obtained [134]. Owing to the vacuum-assisted filtration and sedimentation, the green particle density is relatively high and thus such layers can be sintered at the chosen temperatures to ideal densities. This ensures good gas-tightness, which is one of the basic characteristics an SOFC electrolyte must fulfil.

Up to now the layer quality has been excellent. The major drawback of this technique is that it is less suitable for being introduced into an industrial production line. This is especially true for the planar structures which need to be handled many times (application to the porous support, sealing to the top side by e.g. a rubber gasket, removing the sealing and taking off the coated half-cell). For ease of automation, other techniques like SP or spraying have obvious advantages, and, thus, VSC is still only performed at R&D institutes and not in industry.

Roller/curtain coating While slip casting is mainly a lab-scale technology, SP and spray coating are well established for industrial applications. With respect to fabrication lines, tape casting would be the first choice as a substrate manufacturing techniques. Consequently, also a continuous coating technology would be of great interest. Spray coating is such a continuous technique but, as mentioned above, it suffers from overspray, and SP needs intermediate (automatic) handling for placing and removing the substrate between printing. Two in-line coating technologies are roller coating or curtain coating [155]. In roller coating, the suspension is moved from a reservoir via various intermediate rollers (typically made of metal and coated by a polymer) to a coating roller. The substrate moves on a support through the coating roller, and the suspension is coated while it passes the roll. The layer thickness can be varied by adjusting the distance between the substrate and the coating roller, the suspension viscosity and the through-pass speed. Typical layer thicknesses (final fired state) are in the range of 5–50 μm. If holohedral layers are coated (e.g. anode and electrolyte on anode support), then there is some 'overspray'. This is the suspension which passes on the right and left side of the substrate. This overlapping suspension can easily be collected by a basin under the rolling machine (it is advantageous if the bottom of the transporting support is made of a mesh or sieve structure; thus, the overlapping suspension can pass through and be collected). For these types of coating, there is no overlapping suspension before and after the substrate. By contrast, if layers which do not completely cover the component are to be applied (e.g. cathode on electrolyte), then a surrounding rim of electrolyte is necessary to be applied over the sealing material which connects the cell to the frame and ensures gastight sealing between the two atmosphere. The overlapping suspension can be collected as described above. Figure 6 illustrates the basic coating principle. For coating by rollers, the major prerequisites are planar, even substrates, because normally the coating roller must have an exact diameter to achieve good homogeneous layer thickness. If the substrates are bent and elastic, the coating roller can level them during passing, but the risk of cracking is evident.

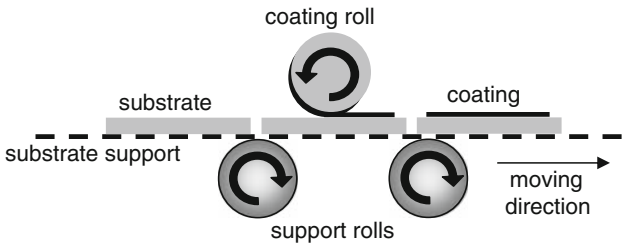

Fig. 6 Roller coating of functional layers

Another possibility for holohedral coatings is the so-called curtain coating. Here, the suspension is not coated by a roller but moves downwards as a continuous curtain (comparable to a waterfall) from a reservoir. The components to be coated are transported in the same way as in roller coating. Also the overlapping suspension (here on all four sides) is collected as mentioned above (see Fig. 7). With this technique, no structured or non-holohedral layers can be applied. However, if non-holohedral layers are to be coated, then the parts of the component which are not to be covered need to be masked before coating. After the coating step, the mask must be removed or, for example, burnt off.

Up to now, only first attempts have been made at using those highly automated mass fabrication coating processes [156]. The first anode-supported SOFCs manufactured by roller coating show acceptable current densities of approximately 1 A/cm^2 at 800 °C and 0.7 V in single cell testing with hydrogen and air (cell size 50 × 50 mm^2) with LSM/8YSZ cathode and LSM current collector. Typical values of such kinds of cells are in the region of ~1.5 A/cm^2. The lower current densities are attributed to

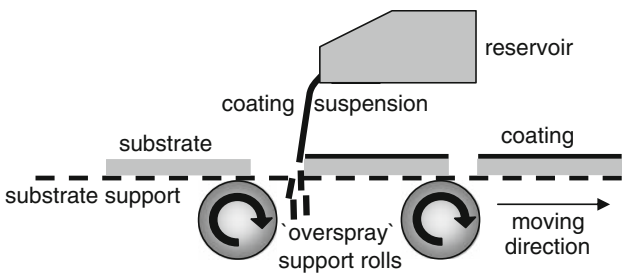

Fig. 7 Curtain coating of functional layers

as yet poorly adapted anode and electrolyte thicknesses (~>10 μm) and insufficient microstructure of the anode. However, in principle there are no major objections to these mass fabrication techniques. If SOFCs enter the mass market, then such technologies will be applied in the future for cell manufacturing.

Dip, spin coating (sol–gel) The need to reduce operating temperatures (from 800–950 to 650–750 °C) also necessitates thinner functional layers to minimise ohmic internal losses. Layer thicknesses of ~5–100 μm can be manufactured by 'classical' ceramic powder technology. If thinner layers are to be applied, then two parameters must be adapted: first, the support must be adapted to thinner structures, which means that the surface roughness and the particle and pore sizes must be reduced (a 1-μm thin layer on a support with particle sizes of 5–10 μm is geometrically impossible or needs great effort, including, for example impregnation with a resin to close the pores; during the ongoing manufacturing steps, the resin needs to be burnt off). Therefore, the basic particle size distributions in the suspensions, slips or pastes tend to be reduced from micro-sized to sub-micro- or nano-sized. This tendency consequently leads to the second parameter, which requires greater efforts in suspension stabilisation because smaller particles tend to form agglomerates, aggregates or to separate more easily. Another possibility of minimising the layer thickness is the use of sol–gel-based techniques. In the sol–gel, the oxides are in a precursor stage and are converted into the oxidic phase during temperature treatment. The basics of sol–gel technology can be found in [157, 158]. The use of this technique for SOFC applications is described in [140–146]. Coating with sol–gel layers can be done in principle by various techniques, e.g. SP roller coating, spraying, and also with dip and spin coating. The coating medium itself can be a pure gel or a mixture of a gel and an oxidic powder phase; in the latter, the gel acts as a kind of binder during manufacturing and the oxide precursor, which forms very small particle sizes (nm range), can act as an aid during sintering to reduce the sintering temperature due to the high sintering activity (excellent surface to volume ratio).

The dip-coating process is applicable to planar or three-dimensional structures. Normally, it is easier to coat porous substrates because of the capillary forces which support the adhesion of the coating than to coat dense structures. Here, the risk of drain-off due to unadapted adhesion behaviour and suspension viscosity is higher. Typical industrial applications are the coating of crockery with glazes or the metallisation of CDs with a reflective layer covered subsequently by e.g. dip or spin coating layers.

The substrates to be coated can be covered completely during dipping or partly by masking the parts which are not to be coated. After coating, the masks must be removed or burnt off. Typical layer thicknesses with powder-based suspensions range from 2 to 10 μm and with sol–gel-suspensions from 10 nm to 2 μm. The dipping itself can be done once or in multiple steps. Normally a drying or calcination step is inserted between multiple coating steps. Especially the quality (e.g. gas-tightness or surface roughness) of the thinner layers depends strongly on the surface quality of the substrate (see above). If multiple coating steps are needed to ensure layer quality, then the technology is more applicable on the laboratory scale, but if the coating can be done in one step, then it is industrially applicable. The major parameters during dip-coating are the suspension viscosity (which governs the layer thickness), the time of coating, the powder loading of the suspension, the coating temperature (at ambient or slightly enhanced temperatures; also affects viscosity) and the speed with which the part is moved through the suspension. Figure 8 shows schematically two possible types of dip-coating (vertical and horizontal).

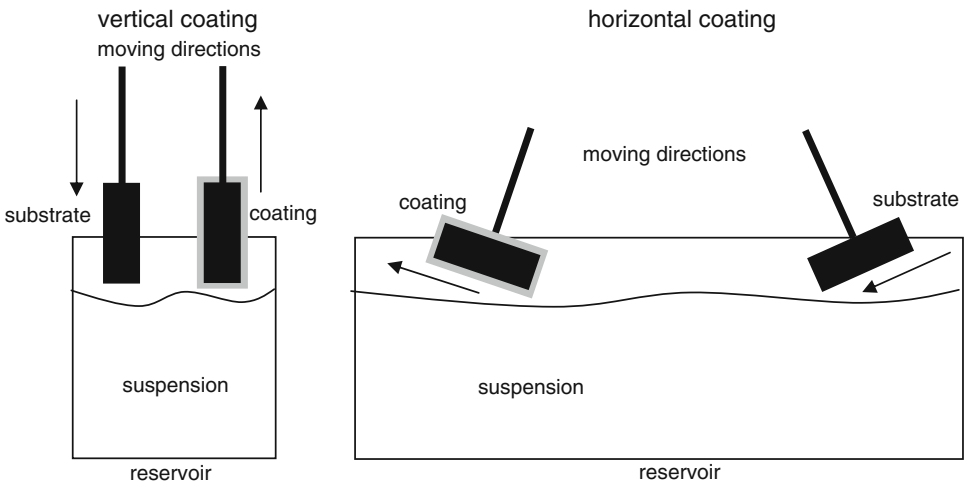

Fig. 8 Types of dip coating

The spin coating process depends, from the suspension point of view, on the same factors as the dip-coating. However, here, the machine parameters play a more important role. The layer is formed during high-speed turning of the planar substrate with the suspension positioned on top of the substrate. The spinning speed (in addition to the suspension viscosity and the adhesion force of the suspension on the substrate) influences the layer thickness. By enhancing the spinning speed, the layer becomes thinner. While for dip coating hardly any unnecessary suspension is left, like the spraying technique, spin-coating produces an overspray. This is the suspension which is moved outwards from the centre to the substrate rims and is spun off. However, the overspray can be collected and re-dispersed. Spin-coating suspensions can be also made of pure powder suspensions as well as sol–gel suspensions and mixtures thereof. Examples of the use of spin-coating for SOFCs are the application of sol–gel electrolyte layers on anode-supported SOFCs [141–144]. Here, spin or dip coating compete with other thin film techniques as described in "Cathode" section.

Up to now, both technologies have been used on the laboratory scale for SOFCs, but they have the potential to be industrialised only if they can be incorporated into a production line, as, for example, in the semi-conductor industry.

Table 3 lists the ceramic coating technologies, typical layer thicknesses and their industrialisation status.

The application of the coating technology for mass production of SOFCs will strongly depend on (a) the industrialisability of the technique, (b) its costs and (c) the obtained or desired film characteristics. In some cases, especially requirements (a) and (c) could be conflicting. Thus, in the application field SOFC, which is sometimes a better technology with respect to film quality, will be replaced by a technique which is more easily incorporated into a production line. Slip casting and SP can be mentioned as an example. Up to now, vacuum slip casting has provided high-quality electrolyte layers with good adhesion, microstructure, reproducibility, thickness and gas-tightness, but it is impossible to industrialise it. Therefore, it will be replaced by SP which is easier to incorporate into a production line, but has the drawback of needing to change the mesh after several coatings and a layer quality which is not yet as good as VSC.

At this point, it must be pointed out that not only will the substrate and coating technologies play a key role during fabrication and industrialisation of SOFCs, but sintering also will remain a crucial parameter. The number of sintering steps needed, the sintering temperatures and the furnaces used will also influence cell quality and costs. The reduction of the number of sintering steps correlates directly with the manufacturing costs, and continuous furnaces will be preferable to batch furnaces. In order to ensure high power output for the cells, it seems that at least two sintering steps are needed: a first step at higher temperatures for the substrate (ESC) or the substrate–anode–electrolyte unit (ASC) to ensure electrolyte gas-tightness, and a second step to apply the electrodes (ESC) or the cathode (ASC). Typical sintering temperatures for the electrolyte material are 1400 °C, and especially the cathode materials do not withstand temperatures above 1200 °C: Either they are highly densified, which results in less current density, or they decompose and thus lose their physical characteristics. Efforts have been made in recent years with co-firing especially of the substrate, anode and electrolyte [159–161].

More literature about ceramic manufacturing technologies, some focusing on SOFCs can be found in [135, 155, 162–165].

Thermal spraying methods

The basics of thermal spraying are described in various books and review articles [44, 166–168], including in part application to SOFC. Thus, in this article only the special application of plasma spraying to SOFCs will be described. Plasma spraying is mostly applied to metal-supported SOFCs (MSCs) because metallic supports cannot be coated by ceramic coating techniques and subsequent sintering at high temperatures (>1200 °C) under oxidative conditions. The metal support will oxidise, and if the sintering regime is long enough, then not only will, for example, chromia layers be formed (which would not be a crucial problem

Table 3 Ceramic coating techniques and some parameters

Technique	Typical film thickness (after sintering)	Industrialisation status according to SOFC
Screen printing	5–100 μm; but only discrete thicknesses (depending on mesh characteristics used)	Established
Spraying	5–100 μm	Established
Slip casting	1–20 μm	Lab scale
Roller, curtain coating	5–20 μm	Lab scale to commercial scale
Dip-, spin coating	2–10 μm for powder-based and 10 nm to 2 μm for sol–gel-based	Lab scale

because they form anyway during operation), but also iron-oxide layers (including the risk of break-away corrosion), and an interdiffusion between the steel and the anodic nickel will change the material properties of both metals and lead to austenitisation of the ferritic steel and reduction of the catalytic activity of Ni. Thus, plasma spraying without any high-temperature sintering as a post-coating step is of interest.

Atmospheric plasma spraying (APS)

Thermal coating by plasma spraying at ambient pressure is mostly used for oxide coatings. Typically a powder with an agglomerate size in the range of some tens of micrometers is used. The powder agglomerate diameter mainly depends on flowability in pressure conveying. Smaller powder sizes tend to form bigger agglomerates and loose flowability; bigger powder particle sizes need higher temperatures or longer retention times within the plasma to be completely melted. These requirements for the powder limit the layer thickness that can be coated. Normally, layer thickness for plasma spraying is between $\sim$40 and 300 μm. Thus, thin films such as 2–10 μm thick electrolytes or electrodes cannot be applied by conventional APS. Another limitation is the substrate to be coated. Because during plasma spraying, the sample to be coated is heated by the plasma flame high temperature gradients that form not only in the *z*-direction but also in the horizontal direction. Ceramics mostly suffer from relatively poorer thermomechanics, and especially thermal gradients promote stresses in the ceramics in excess of their strength, thus leading to substrate cracking. Therefore, plasma spraying is mostly used for metal-supported SOFCs. Here, all the functional layers, electrodes and electrolyte, can in principle be coated. However, during APS there is a risk of oxidising the metal support. The adaptation of the spraying parameters (spraying distance, spraying speed, type of support gas, heating of the substrate etc.) strongly influences the quality of the coating and also of the support. In contrast to Schiller and coworkers [169, 170], who had long experience with vacuum plasma spraying of SOFCs, the group of Vaßen and coworkers tried to apply APS to SOFCs [44, 171, 172]. The latter authors showed that in principle APS is applicable to metal-supported SOFCs based on a support made of Crofer22APU. The current density for single cells reached values of up to $\sim$1 A/cm^2 at 800 °C, 0.7 V with air as oxidant and a mixture of hydrogen with 3% water vapour as fuel. Those values are roughly one-third less than those obtained with typical anode-supported cells but very encouraging. Three drawbacks can be seen at the moment for the APS coatings:

1. The electrolyte layer, which needs to be gas-tight, shows some porosity thus leading to reduced open circuit voltage (OCV) values; this is an indication that the electrolyte is not completely dense. This can be confirmed by measuring the helium leak rate. Typically, anode-supported cells with layers applied by ceramic technology and sintering reach He leak rates of 10^{-6} hPa dm^3/(s cm^2) in the oxidised state of the substrate and the anode, and roughly one order of magnitude higher values in the reduced state [120]. The leak rates measured for the metal-supported plasma-sprayed cells is in the range of 10^{-2} hPa dm^3/(s cm^2) [44]. This results in gas leakage and thus in reduced OCV values. The lower OCV is not a problem for single-cell testing, because this is a short-term measurement, but for stack operation, a permanent leakage between the tow atmospheric compartments leads to an internal gas crossover, and this may result in damage to the electrode (either re-oxidation of the anode or deterioration of the cathode) and/or loss of power, both leading to high degradation rates.
2. The electrodes should be open-pored and show a high number of three-phase boundaries (TPBs). Therefore, a mixture of anodic or cathodic materials needs to be plasma-sprayed. Unfortunately, the microstructure of the manufactured cells shows rather poor porosity, for example horizontal splat pores typical of plasma spraying and poorer interpenetration of the two electrode materials (e.g. NiO + YSZ or LSM + YSZ). Both powders have different physical characteristics (melting point, surface area, materials density etc.) and were thus melted and transported within the plasma flame in a different manner. Therefore, a major power limitation for APS-coated SOFCs refers to non-optimal electrode microstructure.
3. Owing to the flowability of the powders and their underlying particle size distribution, the layer thickness obtained by APS is relatively thick. This results in high intrinsic ohmic losses and subsequently in low power density.

All these three factors limit the power output and the lifetime, i.e. the degradation rate, of a cell or a cell within a stack. However, owing to the advantages of metal supports (re-oxidation tolerance, costs and low-temperature application), coating by plasma spraying is still of great interest, and many R&D groups worldwide are working on this subject.

Vacuum plasma spraying (VPS)

Besides APS, plasma spraying at low pressure is of interest. Typically, VPS is used to coat metallic layers, e.g. bond coats for thermal and environmental barrier coatings [173].

However, great efforts have been taken to apply VPS to SOFCs [169, 170]. The main advantage of VPS in comparison to APS is that thinner layers with a denser microstructure (especially for the electrolyte) can be obtained. For example, DLR has developed an SOFC based on a metal support (Crofer22APU) by spraying the anode, the electrolyte and the cathode using VPS. The basic problem in applying VPS to SOFC is that typically two transport gases, one usually argon and the second hydrogen, are used. By using a strong reducing gas such as hydrogen, especially the perovskites are destroyed by decomposition. Thus, a different second carrier gas needs to be used (e.g. nitrogen, helium). This requires the adaptation of the spray process to each SOFC functional layer to reduce the consequences of using the spraying equipment at suboptimal parameters. As DLR has shown [169], the use of VPS for all functional layers leads to cells with good current densities, and also stacks have been manufactured and tested. The measured current densities for single cells are in the range of 300 mA/cm^2 at 800 °C and 0.7 V with air and a hydrogen/nitrogen mixture (12.57 cm^2 active area), and in stack tests, 270 mA/cm^2 was obtained at 800 °C (4-cell stack with 125 cm^2 active area; hydrogen and air). MSCs still suffer from higher degradation rates (compared to anode- or electrolyte-supported SOFCs) and incomplete electrolyte density, thus involving the risk of electrode destruction. The main purpose of using metal-supported SOFCs is to lower the operating temperature from typically 900–950 °C for ESCs and 750–800 °C for ASCs down to temperatures below 700 °C. The reduced operating temperature may be beneficial for the long-term behaviour of materials for the metallic interconnects and the cells.

Low-pressure plasma spraying (LPPS)

Besides the 'classical' VPS LPPS also has become attractive in recent years. LPPS operates at lower pressure values than VPS (VPS ~ 10–100 hPa, LPPS < 10 hPa). The main advantage of LPPS compared to VPS is a longer plasma flame (because of the lower pressure), which results in longer dwelling times for the powder within the plasma, and in a larger circle which coats the substrate. Thus, the thermal gradients are less pronounced, and the coating time is reduced because fewer meanders are needed forcompletely coating the substrate.

Up to now, there are only a limited number of publications concerning the application of LPPS to SOFC [174–176], but the technology is of extreme interest due to its advantages compared to VPS. In none of the mentioned references were the real cells fabricated and, therefore, no details about cell characteristics could be presented. Those authors deal with coating parameters, microstructural investigations of the coated layers and the influence of the spray parameters and powder characteristics on layer morphology. Especially electrolyte and electrode layers are described in [174, 175] and insulation layers for metallic SOFC components in [176].

Suspension plasma spraying (SPS) and high velocity oxy-fuel spraying (HVOF)

In order to reduce layer thickness during plasma spraying, novel techniques such as SPS and HVOF have been applied for SOFC production. In SPS, not a pure powder but rather a liquid suspension transporting a powder fraction of small particle sizes (sub-μm or nm) is introduced into the plasma flame. Because of the smaller particle sizes, the film thicknesses obtained are also thinner than with APS and VPS/LPPS. Ghosh and coworkers [177–179] have been working with SPS and HVOF for SOFC for approximately three years. Anode layers (composed of NiO-SDC, samaria-doped ceria) were deposited on a porous metal support based on Hastelloy X by SPS. Subsequently, a pure SDC electrolyte layer was deposited the same way. As the cathode material a mixture of SDC and a samaria-tin-cobalt-oxide was screen printed on the electrolyte. The electrochemical testing of such button cells (active area 0.34 cm^2) reveals current densities of ~150 mA/cm^2 at 700 °C and 0.7 V. The functional layer thicknesses were 20–30 μm each (anode, electrolyte). SEM characterisation still shows residual porosity in the electrolyte, thus leading to reduced OCV values. The cathode thickness is roughly 30 μm. The results show that some study remains to be done to increase the power output to typical values obtained with APS or VPS, but the tendency towards lower layer thicknesses to reduce the intrinsic ohmic losses is a step in the right direction. Whether SPS and HVOF have the ability to replace APS or VPS depends on the results obtained (leak rates for the electrolyte, OCV values, current density, degradation rates) and also on the manufacturing costs. The main advantage of APS is that there is no need for a vacuum chamber, and, thus, the investment costs are relatively low compared to the other plasma-spraying techniques. Table 4 compares the thermal-spraying

Table 4 Thermal coating techniques and some parameters

Technique	Typical film thickness	Industrialisation status according to SOFC
Atmospheric plasma spraying	50–300 μm	Lab scale
Vacuum plasma spraying	30–150 μm	Lab scale
Low-pressure plasma spraying	20–100 μm	Lab scale
Suspension plasma spraying and high-velocity oxy fuel spraying	5–50 μm	Lab scale

techniques with respect to their coating thicknesses and industrialisation status.

Gas phase deposition technologies

The coating technologies of the preceding sections can be divided into processes where solid material is directly processed (e.g. screen printing), and those in which constituents of the latter material are in a liquid phase (e.g. thermal spraying, sol–gel precursors). This section now focuses on deposition technologies where coatings are applied from a gas phase.

Physical vapour deposition

Physical vapour deposition (PVD) essentially means the transport of material from a condensed matter phase via a gas phase towards a 'cold' substrate where the material condenses. In general, solely the physical state (solid, liquid, gaseous) is changed, not the material itself. Different methods have been developed to transfer material into the gas phase: examples are thermal evaporation or sputtering.

It is interesting to note that W.R. Grove, who is regarded as the inventor of the fuel cell [180], described the phenomenon that is known today as sputtering, for the first time in 1852 [181].

Evaporation methods In general, evaporating material means putting the material into a gas phase by transferring heat to the material. The simplest way to do this is heating the material in any kind of furnace. In this case, however, the furnace must withstand the temperatures that are necessary to obtain a considerable vapour pressure of the material to be evaporated (often more than 1000 °C). Therefore, more sophisticated heating methods have been developed to heat the material (the 'target') without heating the crucible containing the material. Examples are given in the following.

During arc evaporation, electrical energy is converted into heat at the sample surface by an electric arc. This technique implies that a conductive material is to be evaporated. Laser ablation is a process whereby the electromagnetic energy of the laser light is used to quickly evaporate material. At high laser intensity, the material can even be ionised. The stoichiometry of a layer made by laser ablation is generally very close to that of the target due to the fast evaporation. However, this method requires materials which can absorb the laser light. Electron-beam evaporation sources use the kinetic energy of electrically accelerated electrons to transfer material to the gas phases (see Fig. 11b). Virtually all materials can be electron-beam evaporated. However, the stoichiometry of the layers of a multi-phase material may differ from the target composition due to different partial pressures of the constituents of the target [182].

Allthe above advanced technologies that they have in common is that the material is typically evaporated from a small spot. This spot has to be scanned along a large target, or the sample has to be moved, or the distance between target and sample has to be so large as to evenly coat large samples. The coating procedure is basically a line-of-sight process, which means that the vapour species are supposed not to scatter at each other or at other gas atoms, and to move in a ballistic manner to the sample. Steep edges or undercuts on the sample surface are, therefore, very difficult to coat.

Electron beam evaporation has been used to deposit thin electrolyte films for SOFCs [183, 184]. Figure 9 gives an example of an electrolyte made by EBPVD and electrochemical data of this type of fuel cells. A composite of yttria-stabilised zirconia (YSZ) sandwiched in between two layers of gadolinium-substituted ceria (CGO) was deposited on an anode substrate manufactured by a pressing method (see substrate "Pressing methods" section) and an anode applied by vacuum slip casting as described in the "Slip casting" section. The deposition temperature during electron beam evaporation was 800 °C. No additional

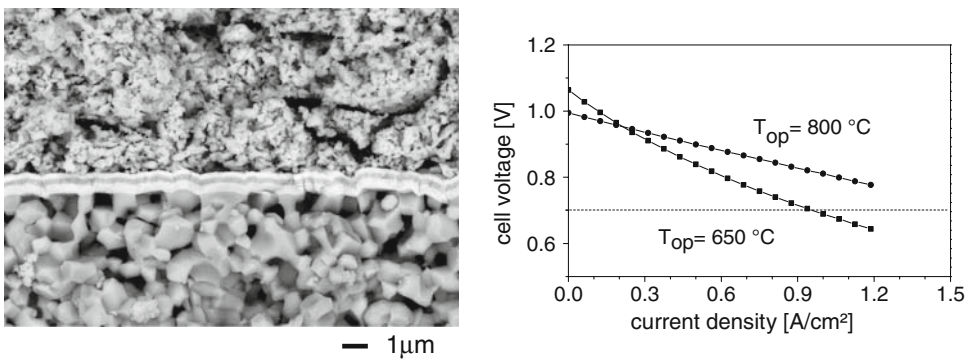

Fig. 9 Cross-sectional fracture surface of an SOFC with an EB-PVD electrolyte layer (*left*) and current–voltage curve of this type of cell for different operating temperatures with gas flows of 1000 mL/min air and hydrogen (incl. 3 vol% water), respectively (*right*); see text

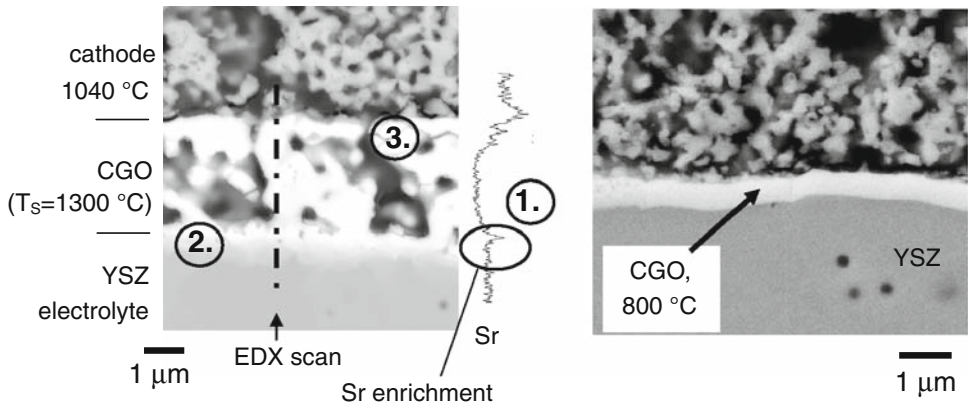

Fig. 10 Comparison of a screen-printed (*left*) and a PVD CGO layer (*right*) for SOFCs; see text. The cathode was sintered at 1040 °C

sintering step was necessary to obtain sufficient gas-tightness. A cathode of $La_{0.58}Sr_{0.40}Fe_{0.8}Co_{0.2}O_{3-\delta}$ (LSFC) was applied by SP and sintered at 1040 °C. Details concerning the measurement of the electrochemical performance can be found in [185].

Another application of EB-PVD in SOFCs is the deposition of diffusion barrier layers: cathode materials like LSFC and YSZ as electrolyte material create insulating layers at temperature of 800 °C and above. Therefore, compatible, thin, dense, ion-conducting barriers are necessary. CGO is, in general, a suitable material. However, it has been proved that screen-printed and subsequently sintered CGO layers do not usually attain full density on anode-supported half-cells with densely sintered YSZ electrolytes (Fig. 10). With EB-PVD, on the other hand, it was possible to achieve apparently dense CGO layers. SOFCs with CGO layers made by EB-PVD exhibit considerably higher performance than those with screen-printed CGO layers [186], which is attributed to the following reasons (Fig. 10): (1) the Sr diffusion from the cathode to the electrolyte (thus forming strontium zirconate) is more effectively inhibited due to the higher density of the CGO layer; (2) due to the reduced application temperature, the detrimental interdiffusion reaction of CGO and YSZ, which have a similar crystal structure, is minimised; (3) assuming that the dominant conduction path for oxygen ions through CGO is not surface conduction, the sponge-like structure of the screen-printed CGO layer increases the resistance, and the effective contact between CGO and cathode and CGO and electrolyte, respectively, seems to be better for the fuel cell with a PVD CGO layer.

Sputtering During sputtering, ions, which are accelerated by an electric field, hit the surface of the sputter target and, thus, eject small species (atoms, ions or clusters of these) from the target (Fig. 11a). Such an arrangement can be easily extended to large target sizes as well as large sample sizes.

The directional distribution of particle flux from the surface follows a cosine law, similar to the distribution of evaporation sources. However, with a large sample facing towards a large target, each point of the target serves as a

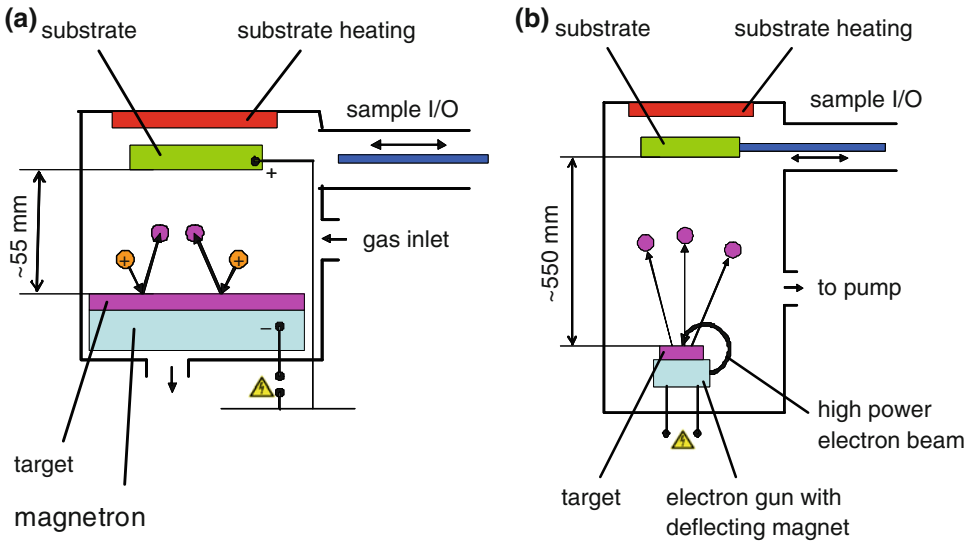

Fig. 11 Sketches of physical vapour deposition methods: **a** In a magnetron sputtered energetic argon ions from a plasma are used to bring target material into the gas phase. **b** Electron beam evaporation (EB-PVD) uses a focused electron beam to melt and evaporate target material

spot source with a cosine distribution of a particle flux, and each point of the sample surface gathers material from many spot sources located at different positions. Therefore, the coating of edges is better for sputtering compared to the single spot source evaporation processes. Nevertheless, it is also a line-of-sight process. A disadvantage of sputtering is the relatively low deposition rate compared to, for example, evaporation processes.

Around 1990, the first attempts to introduce sputter processes for SOFCs were reported, mainly for the fabrication of dense electrolytes [187, 188].

Chemical vapour deposition

During chemical vapour deposition, or CVD, a chemical reaction takes place in the gas phase or on the surface of the sample to be coated: The starting materials, often called 'precursors', are chemicals that can be more or less easily transferred into the gas phase, i.e. gaseous materials or materials with a high vapour pressure. Theses gaseous precursors diffuse to the sample and then react, thus creating the desired material (for a general introduction see [189]). As an example, zirconium chloride ($ZrCl_4$), yttrium chloride (YCl_3) and water (H_2O) can be used to make YSZ (Fig. 12). The reaction proceeds according to the following equations:

$$2\mathrm{MeCl}_y + y\mathrm{H_2O} \rightarrow 2\mathrm{MeO}_{y/2} + 2y\mathrm{HCl}$$

$$4\mathrm{MeCl}_y + y\mathrm{O_2} + 2y\mathrm{H_2} \rightarrow 4\mathrm{MeO}_{y/2} + 4y\mathrm{HCl}$$

where Me is the cation species (zirconium and/or yttrium), and y is the valence associated with the cation. The position where the reaction takes place can be controlled either by the sample temperature (higher than the decomposition temperature of the precursors), by a plasma near the surface to be coated ('plasma-assisted' or 'plasma-enhanced' CVD: PA-CVD or PE-CVD) or by the flow of gases which have to react with each other. In Fig. 12, the purpose of the gas flow is to close the pores in the anode layer, preferentially on top of the anode. A variant of the CVD process is also shown in Fig. 12: In this case, the pores are completely closed by the CVD process, and further growth of the layer is possible due to the ionic conductivity of YSZ. Water releases oxygen ions at the TPB *gas compartment–anode–electrolyte*, the ions move to the surface facing towards the gas flow of the zirconium- and yttrium-containing precursors and then react (*electrochemical CVD*, or EVD).

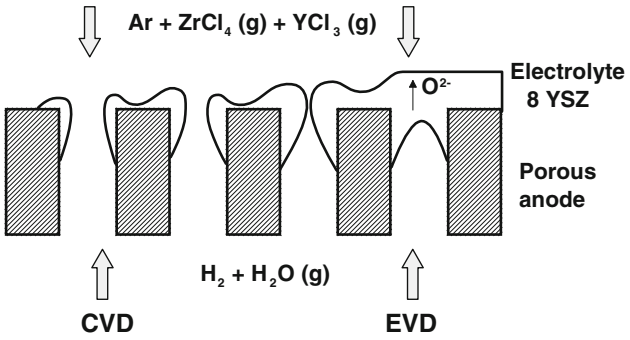

Fig. 12 Sketch of the CVD process for the fabrication of yttria-stabilised zirconia (YSZ)

Metal–organic precursors usually have lower decomposition temperatures than, for instance, chloride-based precursors (*metal–organic CVD*, or MO-CVD).

Another variant of the CVD process is *atomic layer deposition* (ALD). Normally, during CVD, the amount of precursor in the gas phase near the sample determines the growth rate of the layer. During ALD, however, the reaction is controlled by the absorption of material on top of the sample surface. In other words, only one monolayer of a precursor adsorbs onto the surface, the atmosphere with this precursor is subsequently pumped off, and then the second precursor necessary for the reaction is put into the reaction chamber and reacts with the adsorbed precursor. As a result, a monolayer of material is created [190].

The CVD processes are mainly diffusion controlled and are, therefore, in contrast to PVD, not line-of-sight processes, and can also coat inner surfaces of open pores, for instance. This is the case especially for ALD processes.

However, one major problem in CVD concerns the precursor materials. Suitable precursors are difficult to purchase for certain processes, and they are generally expensive.

Electrochemical vapour deposition has been used, for instance, by (Siemens-) Westinghouse for coating of tubular cathode-supported cells with dense electrolyte layers as shown in Fig. 12. YSZ films of about 40 μm in thickness were deposited by the above-mentioned reaction and in addition by

$$2\mathrm{MeCl}_y + y\mathrm{O}^{2-} \rightarrow 2\mathrm{MeO}_{y/2} + y\mathrm{Cl_2} + 2y\mathrm{e}^-$$

$$y\mathrm{H_2O} + 2y\mathrm{e}^- \rightarrow y\mathrm{O}^{2-} + y\mathrm{H_2}$$

The process led to sufficiently gas-tight YSZ layers, but the cost for the process was regarded as too high [191, 192].

Microstructure

The functional principle of a fuel cell demands a microstructure of cathode, anode, and electrolyte. The electrolyte's task is to separate the two gas compartments for fuel gas and oxidant gas, and hence it has to be gas-tight. Therefore, the electrolyte layer must be dense. With a given bulk ion conductivity of the material, the electrolyte

layer can be as thin as possible to reduce the electrical resistance—as long as the gas-tightness is maintained (for this, it is assumed here that the electrolyte does not act as a mechanical support).

The electrodes could—in principle—be ultra-thin dense layers, provided that the electronic and ionic conductivity and the catalytic activity for the corresponding electrochemical reactions are arbitrarily high. However, such materials are not available yet, and alternative microstructures are used in practice. For both the electrolyte and the electrodes, the microstructure obtained (dense, porous fine or porous coarse) is a combination of physical and chemical properties of the materials themselves, the manufacturing technology (thermal, wet chemical, physical, chemical deposition technique) and the subsequent thermal treatment (atmosphere, temperature, time, rates). This interaction between the process technology described in the preceding sections and materials on the microstructure of the electrodes are now presented in more detail.

For the electrochemical reaction, three requirements have to be simultaneously fulfilled: there must be gas available as well as an electron-conducting phase and an oxygen ion-conducting phase. (Therefore, this region is commonly called the three-phase area or three-phase boundary.) Figure 13 shows this for cathodes. On top of an electrolyte layer, a cathode made of a material with perovskite crystal structure consisting of $La_{0.65}Sr_{0.3}MnO_3$ (LSM) is applied, which is a good electron conductor but a poor ion conductor [193]. It has to be an open-porous structure, which means that the single pores are interconnected to allow a gas flow from the outer gas compartment to the cathode–electrolyte interface. The area where gas, electron-conducting and ion-conducting phases simultaneously appear is located immediately adjacent to the electrolyte surface. Since the cathode material is a poor ion conductor, a major part of the cathode material does not contribute to the electrochemical reaction. However, it should be noted that, in some references, it is stated that there is also oxygen diffusion in the cathode material during operation of the fuel cell due to the creation of oxygen defect sites by the overpotential [194, 195].

One route to overcoming this obstacle is to mix the cathode and electrolyte material in the vicinity of the electrolyte layer (Fig. 13, right) [196]. A significant extension of the three-phase area is obtained, as long as open porosity and continuous paths of the electron-conducting and ion-conducting phases are guaranteed.

More sophisticated layers of mixed cathode and electrolyte material are also found in the literature, where a gradual change from 100% electrolyte material/0% cathode material to 0% electrolyte material/100% cathode material was implemented [197]. Care has to be taken with this arrangement since the partial electrochemical reaction $O_2 + 4e^- \rightarrow 2O^{2-}$ requires the coincidence of gas and continuous conducting paths for electrons as well as for ions. If the amount of, for example, electron-conducting material is below a corresponding percolation threshold, electrons cannot be provided to this region, and the partial electrochemical reaction may not take place any more [198].

Another approach is to choose an electrode material that has intrinsic electronic and ionic conductivity, instead of a cathode comprising a mixture of two phases, one of which is electron-conducting and the other ion-conducting (Fig. 14). Thus, the catalytically active area is extended from ‘reaction lines’ to the entire surface of the cathode material.

Perovskites are a material class that can have oxygen-ion conductivity. Their ability to enable the reaction $O_2 + 4e^- \rightarrow 2O^{2-}$ and to conduct oxygen ions varies with composition. Cobalt-based compositions exhibited the lowest overpotential of cathode–electrolyte half-cells; however, they suffered from an adverse reaction with the YSZ electrolyte. Different electrolyte materials are necessary which do not react with this type of perovskite, for instance doped ceria, or composite electrolytes with a top layer of ceria. Manganese-based perovskites were found to be a good compromise between chemical stability in contact with YSZ and electrochemical activity [60].

Both types of cathodes benefit from a large surface area for proper functioning. It is easy to ensure that this area increases with decreasing particle size of the cathode material, and vice versa.

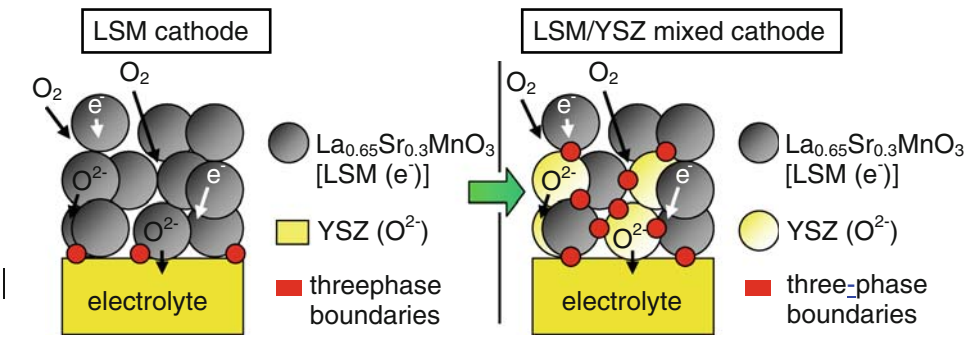

Fig. 13 Sketch of a half-cell comprising an electrolyte and a cathode. *Left*: The cathode is an electron conductor and porous to enable gas feeding, the electrolyte is an ion conductor. *Right*: Increase of the area where the electrochemical reaction $O_2 + 4e^- \rightarrow 2O^{2-}$ can take place (*small circles*)

For ceramic cathodes, cathode powder is typically synthesised, if necessary milled to a certain particle size, and then applied through, for example, printing or painting to the electrolyte and subsequently sintered. The particle size is determined by the initial particle size and the sintering procedure [60]. On the one hand, higher temperatures lead to coarser particles, which is advantageous for enhanced contact between the particles and, thus, for high conductivity, and—in some cases—larger pores for increased gas throughput. On the other hand, the active surface area is reduced, thus leading to a lower effective electrochemical reaction rate. Therefore, the sintering temperature has a direct influence on cell performance (Fig. 15).

The sintering behaviour of materials is not only determined by the particle size, but, of course, also by the material itself. As an example, changes in the composition of perovskite materials—including cation deficiencies on certain lattice sites—can lead to different sintering characteristics. This fact has to be taken into account for assessing the effect of compositional changes in the series of cathode materials under investigation: The influence of the pure material properties and the influence of the microstructure must be distinguished [199–201].

Another fact that has to be taken into account is the thickness of the electrode layer and, for cathodes with more than one homogeneous layer, the ratio of the layer thicknesses. There may not be sufficient three-phase area present if the layers are too thin. Moreover, the in-plane conductance might be too low for proper current collection, which, thus, leads to lower performance [202, 203].

The microstructure is not only important for functional layers, but also for the substrate materials. This is discussed in the following with the example of anode substrates made of nickel (Ni) and YSZ.

Gas permeability and electrical conductivity are crucial for the functioning of an electrode substrate for a fuel cell. Moreover, the thermal expansion coefficient has to be adapted to that of the functional layers.

An open-porous Ni network would fulfil the first two requirements. However, for a matching thermal expansion, and to inhibit too severe sintering, Ni is mixed with YSZ. A continuous framework of YSZ can adapt the thermal expansion to the demands. Roughly, a portion of around one-third of the total volume is necessary for such an interconnected framework, another one-third of Ni to ensure conductivity (above the percolation threshold), and

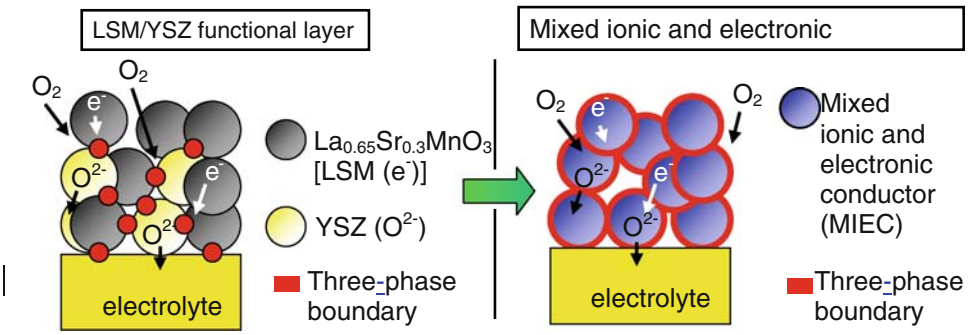

Fig. 14 Change from a heterogeneous cathode material with one electron-conducting phase and one ion-conducting phase to a homogeneous material with so-called 'mixed ionic and electronic' conductivity

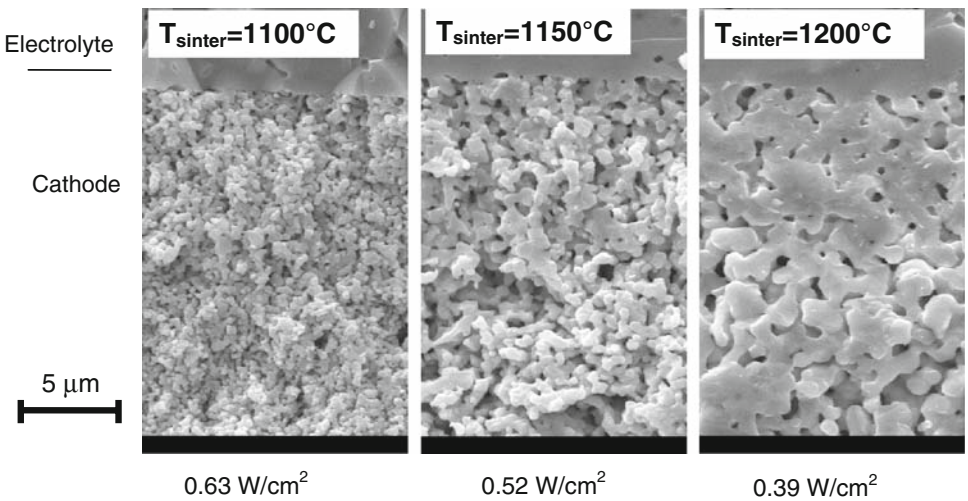

Fig. 15 Scanning electron micrographs of cathodes made of $Pr_{0.65}Sr_{0.3}MnO_{3-\delta}$ sintered at three different temperatures along with the output power at 800 °C and 0.7 V cell voltage of 50 mm × 50 mm cells with an active cathode area of 40 mm × 40 mm operated with 1000 mL/min air and hydrogen, respectively (data taken from [1]). With increasing sintering temperature performance significantly decreased

one-third of the volume for pores for gas permeation. In some applications, higher stability is desired. This can be obtained by a higher volume proportion of YSZ, without changing the ratio of YSZ to Ni (for good conductivity); in other words, the geometric density has to be increased, or a there will be a smaller amount of pores [204]. This may lead to an undesired gas supply shortage during fuel cell operation [205]. Therefore, the thickness of the substrate might be reduced to prevent or to minimise the losses due to low gas permeation.

Another approach is to change the distribution of the Ni in the substrate. The actual percolation threshold strongly depends on the 'type' of distribution of the conductive phase: the percolation threshold for a hexagonal closed package of round mono-modal particles, for instance, differs from that of Ni fibres. Therefore, besides processing substrates on the basis of powder particles, Ni–YSZ substrates have been made by coating the YSZ particle with Ni precursors where the percolation threshold might be shifted to significantly lower values [206, 207].

Conclusions and outlook

A great deal of effort has been invested in solid oxide fuel cells in the past decade. This accounts for the development of high-power materials (especially cathode materials), for the processing of SOFC functional layers for the reduction of materials costs (e.g. for metallic interconnects), and the understanding of microstructural design in the functional layers to enhance power output. Nowadays, sufficient know-how is available to manufacture cells of high power output and low degradation rates with respect to materials and processing technology. Various developers from R&D institutions and also from companies have demonstrated on a laboratory and commercial scale, respectively, the proof of their concepts. Some field tests have already been carried out, but much more testing seems to be necessary to push the SOFCs into a worldwide market. In comparison to other types of fuel cells, SOFCs have a wide range of advantages and thus, in addition to polymer electrolyte fuel cells for portable applications, they could be one of the first types of fuel cells to enter the market.

In the future, study on SOFCs should focus on (a) real operational results obtained by field testing, (b) lowering the manufacturing costs of all components (cells, interconnects, stack, balance-of-plant), (c) understanding degradation mechanisms with respect to materials interaction, fuel contaminations and morphology changes. Especially for stationary applications, a lifetime of more than 40,000 h is envisaged, and thus the degradation rate should be as low as possible, e.g. a voltage loss below 0.25%/1000 h, (d) development of accelerated testing procedures to gain realistic degradation data for lifetime predictions from short-term tests, and (e) development of new materials and concepts for future SOFC applications at lower temperatures (<600 °C using hydrogen or methanol as fuel) or in harsh conditions (reoxidation tolerance of the anode substrate). Therefore, two development lines seem to be proceeding in parallel: testing of the existing stacks and systems and developing new materials, processes and systems for novel application fields for reduced operation temperature and also for high-temperature electrolysis (solid oxide electrolysis cell, SOEC).

Based on these development lines, future work will probably be split into two levels: firstly, on the industrial level, the reduction of materials and manufacturing costs and the assembly of stacks and systems for operational experience combined with the development of accelerated test protocols. This has to be done by cell and interconnect developers, by stack integrators as well as by system suppliers. Secondly, on the R&D level at universities and research institutes, research into the understanding of degradation mechanisms, lifetime modelling and the development of novel materials to overcome the degradation phenomena (if related to materials interactions).

In future, APU applications, e.g. for heavy trucks and leisure (mobile homes, sailing ships), seem to be one of the first markets for SOFCs since the existing stacks and systems fulfil most of the requirements with respect to lifetime (<10,000 h), power density ($\sim$1–1.5 A/cm^2 for the cell) and costs. Applications like household energy supply ($\sim$1 kW_{el}) are on the way and field testing has started, but such applications need more operational results to ensure their applicability, especially with respect to daily, weekly and monthly fluctuations due to energy need and climate. Long-term applications (>5 years) such as decentralised power supply (>100 kW_{el}) will probably be the final field of market entry because of insufficient lifetime (too high degradation rates for existing stacks and systems) and high economic burden and risk.

References

1. Van Herle J, Ihringer R, Sammes NM, Tompsett G, Kendall K, Yamada K, Wen C, Kawada T, Ihara M, Mizusaki J (2000) Solid State Ionics 132:333
2. Singhal SC (1997) In: Stimming U, Singhal SC, Tagawa H, Lehnert W (eds) Proc. 5th Int. Symp. SOFC (SOFC-V). The Electrochemical Society, Pennington, NJ, p 37
3. Tietz F (2003) Mater Sci Forum 426–432:4465
4. Blum L, Meulenberg WA, Nabielek H, Steinberger-Wilckens R (2005) Int J Appl Ceram Technol 2:482
5. Tietz F, Buchkremer H-P, Stöver D (2002) Solid State Ionics 152–153:373
6. Arai H, Eguchi K, Setoguchi T, Yamaguchi R, Hashimoto K, Yoshimura H (1991) In: Grosz F, Zegers P, Singhal SC,

Yamamoto O (eds) Proc. 2nd Int. Symp. SOFC (SOFC-II). Commission of the European Communities, Brussels, p 167
7. Buchkremer H-P, Diekmann U, Stöver D (1996) In: Thorstensen B (ed) Proc. 2nd Eur. SOFC Forum. European Fuel Cell Forum, Oberrohrdorf, Switzerland, p 221
8. Iwata T, Kadokawa N, Takenoiri S (1995) In: Dokiya M, Yamamoto O, Tagawa H, Singhal SC (eds) Proc. 4th Int. Symp. SOFC (SOFC-IV). The Electrochem. Soc., Pennington, NJ, p 110
9. Gardner FJ, Day MJ, Brandon NP, Pashley MN, Cassidy M (2000) J Power Sources 86:122
10. Buchkremer H-P, Diekmann U, de Haart LGJ, Kabs H, Stimming U, Stöver D (1997) In: Stimming U, Singhal SC, Tagawa H, Lehnert W (eds) Proc. 5th Int. Symp. SOFC (SOFC-V). The Electrochemical Society, Pennington, NJ, p 160
11. Tietz F, Dias FJ, Simwonis D, Stöver D (2000) J Eur Ceram Soc 20:1023
12. Christiansen N, Larsen JG (2001) European Patent EP0796827 (B1)
13. Tang E, Martell F, Brulé R, Marcotte K, Borglum B (2003) In: Singhal SC, Dokiya M (eds) Proc. 8th Int. Symp. SOFC (SOFC VIII). The Electrochemical Society, Pennington, NJ, p 935
14. Yokokawa H, Tu H, Iwanschitz B, Mai A (2008) J Power Sources 182:400
15. Shaigan N, Qu W, Ivey DG, Chen W (2010) J Power Sources 195:1529
16. Gong M, Liu X, Trembly J, Johnson C (2007) J Power Sources 168:289
17. Nakayama S, Sakamoto M (1998) J Eur Ceram Soc 18:1413
18. Norby T, Osborg PA (1994) In: Bossel U (ed) Proc. 1st Eur. SOFC Forum. Eur. Fuel Cell Forum, Oberrohrdorf, Switzerland, p 671
19. Gibson IR, Dransfield GP, Irvine JTS (1998) J Mater Sci 33:4297. doi:10.1023/A:1004435504482
20. Badwal SPS, Drennan J (1992) Solid State Ionics 53–56:769
21. Yamamoto Y, Arati Y, Takeda Y, Imanishi N, Mizutani Y, Kawai M, Nakamura Y (1995) Solid State Ionics 79:137
22. Haering C, Roosen A, Schichl H, Schnöller M (2005) Solid State Ionics 176:261
23. Blumenthal RN, Prinz BA (1967) J Appl Phys 38:2376
24. Horita T, Sakai N, Yokokawa H, Dokiya M, Kawada T, Van Herle J, Sasaki K (1997) J Electroceram 1:155
25. Tsoga A, Gupta A, Naoumidis A, Nikolopoulos P (2000) Acta Mater 48:4709
26. Ishihara T, Matsuda H, Takita J (1994) J Am Chem Soc 116:3801
27. Huang K, Tichy RS, Goodenough JB (1998) J Am Ceram Soc 81:2565
28. Huang K, Tichy RS, Goodenough JB (1998) J Am Ceram Soc 81:2581
29. Martin-Sedeño MC, Losilla ER, León-Reina L, Bruque S, Marrero-López D, Núñez P, Aranda MAG (2004) Chem Mater 16:4960
30. Chesnaud A, Joubert O, Caldes MT, Ghosh S, Piffard Y, Brohan L (2004) Chem Mater 16:5372
31. Martin-Sedeño MC, Marrero-López D, Losilla ER, León-Reina L, Bruque S, Núñez P, Aranda MAG (2005) Chem Mater 17:5989
32. Bin Hassan OH, Tietz F, Stöver D (2009) Solid State Ionics 180:831
33. Lacerda M, Irvine JTS, Glasser FP, West AR (1988) Nature 332:525
34. Hosono H, Hayashi K, Kajihara K, Sushko PV, Shluger AL (2009) Solid State Ionics 180:550
35. Purohit RD, Chesnaud A, Lachgar A, Joubert O, Caldes MT, Piffard Y, Brohan L (2005) Chem Mater 17:4479
36. Ishihara T, Arikawa H, Nishiguchi H, Takita Y (2002) Solid State Ionics 154–155:455
37. Jiang SP, Chan SH (2004) J Mater Sci 39:4405. doi:10.1023/B:JMSC.0000034135.52164.6b
38. Tietz F, Dias FJ, Naoumidis A (1998) In: Stevens P (ed) Proc. 3rd Eur. SOFC Forum, vol 1. Eur. Fuel Cell Forum, Oberrohrdorf, Switzerland, p 171
39. Meschke F, Dias FJ, Tietz F (2001) J Mater Sci 36:5719. doi:10.1023/A:1012594406053
40. Steinbrech RW, Caron A, Blaß G, Dias FJ (1997) In: Stimming U, Singhal SC, Tagawa H, Lehnert W (eds) Proc. 5th Int. Symp. SOFC (SOFC-V). The Electrochemical Society, Pennington, NJ, p 727
41. Malzbender J, Wessel E, Steinbrech RW (2005) Solid State Ionics 176:2201
42. Marina OA, Canfield NL, Stevenson JW (2002) Solid State Ionics 149:21
43. Lang M, Henne R, Schaper S, Schiller G (2001) J Therm Spray Technol 10:618
44. Stöver D, Hathiramani D, Vaßen R, Damani RJ (2006) Surf Coat Technol 201:2002
45. Matus YB, De Jonghe LC, Jacobson CP, Visco SJ (2005) Solid State Ionics 176:443
46. Atkinson A, Barnett S, Gorte RJ, Irvine JTS, McEvoy AJ, Mogensen M, Singhal SC, Vohs J (2004) Nat Mater 3:17
47. Jiang SP, Chen XJ, Chan SH, Kwok JT (2006) J Electrochem Soc 153:A850
48. Kurokawa H, Yang LM, Jacobsen CP, De Jonghe LC, Visco SJ (2007) J Power Sources 164:510
49. Fu QX, Tietz F, Sebold D, Tao SW, Irvine JTS (2007) J Power Sources 171:663
50. Kim GT, Gross MD, Wang WS, Vohs JM, Gorte RJ (2008) J Electrochem Soc 155:B360
51. Pillai MR, Kim IW, Bierschenk DM, Barnett SA (2008) J Power Sources 185:1086
52. Ma QL, Tietz F, Sebold D, Stöver D (2009) J Power Sources. doi:10.1016/j.jpowsour.2009.09.075
53. McIntosh S, Gorte RJ (2004) Chem Rev 104:4845
54. Tao SW, Irvine JTS (2004) Chem Rec 4:83
55. Goodenough JB, Huang Y-H (2007) J Power Sources 173:1
56. Sun CW, Stimming U (2007) J Power Sources 171:247
57. Fu QX, Tietz F (2008) Fuel Cells 8:283
58. Minh NQ (1993) J Am Ceram Soc 76:563
59. Jiang SP (2008) J Mater Sci 43:6799. doi:10.1007/s10853-008-2966-6
60. Yamamoto O, Takeda Y, Kanno R, Noda M (1987) Solid State Ionics 22:241
61. Tietz F (1999) In: Vincenzini P (ed) Proc. 9th CIMTEC-World ceramic congress and forum on new materials, vol 24: innovative materials in advanced energy technologies. Techna Publishers S.r.l., Faenza, Italy, p 61
62. Chen CC, Nasrallah MM, Anderson HU, Alim MA (1995) J Electrochem Soc 142:491
63. Sahibzada M, Steele BCH, Zheng K, Rudkin RA, Metcalfe IS (1997) Catal Today 38:459
64. Tietz F, Fu QX, Haanappel VAC, Mai A, Menzler NH, Uhlenbruck S (2007) Int J Appl Ceram Technol 4:436
65. Adler SB, Lane JA, Steele BCH (1996) J Electrochem Soc 143:3554
66. Ullmann H, Trofimenko N, Tietz F, Stöver D, Ahmad-Khanlou A (2000) Solid State Ionics 138:79
67. Takeda Y, Kanno R, Noda M, Tomida Y, Yamamoto O (1987) J Electrochem Soc 134:2656
68. Wei B, Lü Z, Huang XQ, Miao JP, Sha XQ, Xin XS, Su WH (2006) J Eur Ceram Soc 26:2827
69. Bucher E, Egger A, Ried P, Sitte W, Holtappels P (2008) Solid State Ionics 179:1032

70. Shao ZP, Haile SM (2004) Nature 431:170
71. Yan A, Cheng M, Dong YL, Yang WS, Maragou V, Song SQ, Tsiakaras P (2006) Appl Catal B 66:64
72. Bucher E, Egger A, Caraman GB, Sitte W (2008) J Electrochem Soc 155:B1218
73. Martin C, Maignan A, Pelloquin D, Nguyen N, Raveau B (1997) Appl Phys Lett 71:1421
74. Taskin AA, Lavrov AN, Ando Y (2005) Appl Phys Lett 86:091910
75. Kim G, Wang S, Jacobson AJ, Yuan Z, Donner W, Chen CL, Reimus L, Brodersen P, Mims CA (2006) Appl Phys Lett 88:024103
76. Kim JH, Cassidy M, Irvine JTS, Bae JM (2009) J Electrochem Soc 156:B682
77. Ganguly P, Rao CNR (1973) Mater Res Bull 8:405
78. Takeda Y, Nishijima M, Imanishi N, Kanno R, Yamamoto O, Takano M (1992) J Solid State Chem 96:72
79. Skinner SJ, Kilner JA (2000) Solid State Ionics 135:709
80. Boehm E, Bassat J-M, Dordor P, Mauvy F, Grenier J-C, Stevens P (2005) Solid State Ionics 176:2717
81. Munnings CN, Skinner SJ, Amow G, Whitfield PS, Davidson IJ (2005) Solid State Ionics 176:1895
82. Nie HW, Wen T-L, Wang SR, Wang YS, Guth U, Vashook V (2006) Solid State Ionics 177:1929
83. Lalanne C, Prosperi G, Bassat J-M, Mauvy F, Fourcade S, Stevens P, Zahid M, Diethelm S, Van Herle J, Grenier J-C (2008) J Power Sources 185:1218
84. Haanappel VAC, Lalanne C, Mai A, Tietz F (2009) J Fuel Cell Sci Technol 6:041016
85. Anderson HU, Tietz F (2003) In: Singhal SC, Kendall K (eds) High-temperature solid oxide fuel cells: fundamentals, design and applications. Elsevier Advanced Technology, p 173. ISBN 1-85617-387-9
86. Armstrong TR, Stevenson JW, Pederson LR, Raney PE (1996) J Electrochem Soc 143:2919
87. Quadakkers WJ, Piron-Abellan J, Shemet V, Singheiser L (2003) Mater High Temp 20:115
88. Huczkowski P, Christiansen N, Shemet V, Piron-Abellan J, Singheiser L, Quadakkers WJ (2004) Mater Corros 55:825
89. Stanislowski M, Wessel E, Hilpert K, Markus T, Singheiser L (2007) J Electrochem Soc 154:A295
90. Hilpert K, Das D, Miller M, Peck DH, Weiß R (1996) J Electrochem Soc 143:3642
91. Paulson SC, Birss VI (2004) J Electrochem Soc 151:A1961
92. Taniguchi S, Kadowaki M, Kawamura H, Yasuo T, Akiyama Y, Miyake Y, Saitoh T (1995) J Power Sources 55:73
93. Tucker MC, Kurokawa H, Jacobson CP, De Jonghe LC, Visco SJ (2006) J Power Sources 160:130
94. Yokokawa H, Sakai N, Horita T, Yamaji K, Brito ME, Kishimoto H (2008) J Alloys Compd 452:41
95. Menzler NH, Tietz F, Bram M, Vinke IC, de Haart LGJ (2008) Ceram Eng Sci Proc 29(5):91
96. Neumann A, Menzler NH, Vinke I, Lippert H (2009) ECS Trans 25(2):2889
97. Schmidt H, Brückner B, Fischer K (1995) In: Dokiya M, Yamamoto O, Tagawa H, Singhal SC (eds) Proc. 4th Int. Symp. SOFC (SOFC-IV). The Electrochemical Society, Pennington, NJ, p 869
98. Ruckdäschel R, Henne R, Schiller G, Greiner H (1997) In: Stimming U, Singhal SC, Tagawa H, Lehnert W (eds) Proc. 5th Int. Symp. SOFC (SOFC-V). The Electrochemical Society, Pennington, NJ, p 1273
99. Quadakkers WJ, Greiner H, Hänsel M, Pattanaik A, Khanna AS, Malléner W (1996) Solid State Ionics 91:55
100. Larring Y, Norby T (2000) J Electrochem Soc 147:3251
101. Teller O, Meulenberg WA, Tietz F, Wessel E, Quadakkers WJ (2001) In: Yokokawa H, Singhal SC (eds) Proc. 7th Int. Symp. SOFC (SOFC-VII). The Electrochemical Society, Pennington, NJ, p 895
102. Zahid M, Tietz F, Sebold D, Buchkremer HP (2004) In: Mogensen M (ed) Proc. 6th Eur. SOFC Forum, Lucerne, vol 2. European Fuel Cell Forum, Oberrohrdorf, Switzerland, p 820
103. Deng XH, Wei P, Reza Bateni M, Petric A (2006) J Power Sources 160:1225
104. Bertoldi M, Zandonella T, Montinaro D, Quaranta A, Sglavo VM (2004) In: Kilner JA (ed) Proc. 7th Eur. SOFC Forum, Lucerne. European Fuel Cell Forum, Oberrohrdorf, Switzerland, File P0807
105. Yang ZG, Xia GG, Stevenson JW (2005) Electrochem Solid State Lett 8:A168
106. Petric A, Huang P, Tietz F (2000) Solid State Ionics 135:719
107. Donald IW (1993) J Mater Sci 28:2841. doi:10.1007/BF00354689
108. Lahl N, Singh K, Singheiser L, Hilpert K, Bahadur D (2000) J Mater Sci 35:3089. doi:10.1023/A:1004851418274
109. Lahl N, Bahadur D, Singh K, Singheiser L, Hilpert K (2002) J Electrochem Soc 149:A607
110. Yang ZG, Stevenson JW, Meinhardt KD (2003) Solid State Ionics 160:213
111. Gross SM, Conradt R, Geasee P, Shemet V, Quadakkers WJ, Remmel J, Reisgen U (2004) In: Mogensen M (ed) Proc. 6th Eur. SOFC Forum, vol 2. European Fuel Cell Forum, Oberrohrdorf, Switzerland, p 800
112. Haanappel VAC, Shemet V, Vinke IC, Groß SM, Koppitz T, Menzler NH, Zahid M, Quadakkers WJ (2005) J Mater Sci 40:1583. doi:10.1007/s10853-005-0657-0
113. Fergus JW (2005) J Power Sources 147:46
114. Chou YS, Stevenson JW, Chick LA (2002) J Power Sources 112:130
115. Bram M, Reckers S, Drinovac P, Moench J, Steinbrech RW, Buchkremer HP, Stöver D (2004) J Power Sources 138:111
116. Weil KS, Kim JY, Hardy JS (2005) Electrochem Solid State Lett 8:A133
117. Weil KS, Coyle CA, Darsell JT, Xia GG, Hardy JS (2005) J Power Sources 152:97
118. Kuhn B, Wetzel FJ, Malzbender J, Steinbrech RW, Singheiser L (2007) In: Eguchi K, Singhal SC, Yokokawa H, Mizusaki J (eds) Proc. 10th Int. Symp. SOFC (SOFC-X). Nara, Japan. ECS Trans 7(1):413 ff
119. Mistler RE, Twiname ER (2000) Tape casting: theory and practice. The American Ceramic Society, Westerville, OH
120. Mücke R, Menzler NH, Buchkremer HP, Stöver D (2007) In: Kriegesmann J (ed) Technische Keramische Werkstoffe. Verlag Deutscher Wirtschaftsdienst, Chap. 8.5.2.3
121. Menzler NH, Zahid M, Buchkremer HP (2004) In: Kriegesmann J (ed) Technische Keramische Werkstoffe. Verlag Deutscher Wirtschaftsdienst, p 1, Chap. 3.4.6.1
122. Roosen A (2000) Ceram Trans 106:479
123. Bitterlich B, Lutz C, Roosen A (2002) Ceram Int 28:675
124. Christiansen N, Hansen JB, Holm-Larsen H, Linderoth S, Larsen PH, Hendriksen PV, Hagen A (2007) ECS Trans 7(1):31
125. Ramousse S, Menon M, Brodersen K, Knudsen J, Rabbek U, Larsen PH (2007) ECS Trans 7(1):317
126. Tang E, Prediger D, Pastula M, Borglum B (2005) In: Singhal SC, Mizusaki J (eds) Proc. of the 9th Int. Symp. SOFC (SOFC-IX). The Electrochemical Society, Pennington, NJ, USA, p 89
127. Otterstedt R, Rietveld G, Huiberts RC (2005) In: Singhal SC, Mizusaki J (eds) Proc. of the 9th Int. Symp. SOFC (SOFC-IX). The Electrochemical Society, Pennington, NJ, USA, p 476
128. Schafbauer W, Menzler NH, Buchkremer HP (2009) ECS Trans 25(2):649
129. Schafbauer W, Kauert R, Menzler NH, Buchkremer HP (2008) Proc. 8th Eur. SOFC Forum, Lucerne, Switzerland, June 30 to July 4, 2008

130. Voisard C, Weissen U, Batawi E, Kruschwitz R (2002) In: Huijsmans J (ed) Proc. 5th Eur. SOFC Forum, Lucerne, Switzerland, July 1–5, 2002, p 18
131. Brandner M, Bram M, Froitzheim J, Buchkremer HP, Stöver D (2008) Solid State Ionics 179(27–32):1501
132. Crofer22APU Material Data Sheet No. 4046 (2008) ThyssenKrupp VDM, Werdohl, Germany, June 2008
133. Venskutonis A, Kunschert G, Mueller E, Hoehle H (2007) ECS Trans 7:2109
134. Meulenberg WA, Menzler NH, Buchkremer HP, Stöver D (2002) In: Manthiram A, Kumta PN, Sundaram SK, Ceder G (eds) Ceramic transactions: materials for electrochemical energy conversion and storage, vol 127. American Ceramic Society, Westerville, OH, p 99
135. Stöver D, Buchkremer HP, Huijsmans JPP (2003) In: Vielstich W, Lamm A, Gasteiger HA (eds) Chapter 72, Handbook of fuel cells, fundamentals, technology and application, vol 4: fuel cell technology and applications, Part 2. John Wiley & Sons Ltd., p 1015
136. Vora SD (2007) ECS Trans 7:149
137. Minh NQ, Montgomery K (1997) In: Stimming U, Singhal SC, Tagawa H, Lehnert W (eds) Proc. of the 5th Int. Symp. SOFC (SOFC-V). The Electrochemical Society, Pennington, NJ, USA, p 153
138. Ried P, Lorenz C, Brönstrup A, Graule T, Menzler NH, Sitte W, Holtappels P (2008) J Eur Ceram Soc 28:1801
139. Hansch R, Chowdhury MRR, Menzler NH (2009) Ceram Int 35:803
140. Menzler NH, Hansch R, Gaudon M, Buchkremer HP, Stöver D (2005) Mater Forum 29:403
141. van der Donk GJW, Serra JM, Meulenberg WA (2008) J Non-Cryst Solids 354:3723
142. van Gestel T, Sebold D, Meulenberg WA, Buchkremer HP (2008) Solid State Ionics 179:428
143. van Gestel T, Sebold D, Kruidhof H, Bouwmeester HJM (2008) J Membr Sci 318:413
144. van Gestel T, Meulenberg WA, Bram M, Buchkremer HP (2008) CD-ROM Ceram Eng Sci Proc 28(8):37
145. Swider KE, Worrell WL (1996) J Mater Res 11(2):381
146. Lenormand P, Rieu M, Cienfuegos RF, Julbe A, Castillo S, Ansart F (2008) Surf Coat Technol 203(5–7):901
147. Menzler NH, Fleck R, Mertens J, Schichl H, Buchkremer HP (2002) In: Huijsmans J (ed) Proc. of the 5th Eur. SOFC Forum, Lucerne, Switzerland, July 1–5, 2002, p 156
148. de Haart LGJ, Vinke IC, Janke A, Ringel H, Tietz F (2001) In: Yokokawa H, Singhal SC (eds) Proc. of the 7th Int. Symp. SOFC (SOFC-VII). The Electrochemical Society, Pennington, NJ, USA, p 111
149. Bohac P, Gauckler L (1999) Solid State Ionics 119:317
150. Chen CH, Schoonman J (2004) J Ind Eng Chem 10:1114
151. Yamaij K, Negishi H, Horita T, Sakai N, Xiong Y, Yokokawa H (2002) In: Huijsmans J (ed) Proc. 5th Eur. SOFC Forum. European Fuel Cell Forum, Oberrrohrdorf, Switzerland, p 140
152. Sarkar P, Nicholson PS (1996) J Am Ceram Soc 78:1897
153. Moreno R, Ferrari B (2000) Am Ceram Soc Bull 79:44
154. http://www.cerespower.com/
155. Buchkremer HP, Menzler NH (2007) In: Groza JR, Shackelford JF, Lavernia EJ, Powers MT (eds) Materials processing handbook. CRC Press, Boca Raton, FL, USA, p 24-1
156. Büchler O, Bram M, Mücke R, Buchkremer HP (2009) ECS Trans 25(2):655
157. Brinker CJ, Scherer G (1990) Sol gel science. Academic Press, NY, USA
158. Burggraaf AJ, Cot L (1996) Fundamentals of inorganic membrane science and technology, Elsevier Science and Technology Series 4. Elsevier, Amsterdam, The Netherlands
159. Mücke R, Menzler NH, Buchkremer HP, Stöver D (2009) J Am Ceram Soc 92:S95
160. Yoon KJ, Huang W, Ye G, Gopalan S, Pal UB, Secombe DA Jr (2007) J Electrochem Soc 154:B389
161. Yamaguchi T, Suzuki T, Shimizo S, Fujishiro V, Awano M (2007) J Membr Sci 300:45
162. Suzuki M (2003) In: Vielstich W, Lamm A, Gasteiger HA (eds) Chapter 73, Handbook of fuel cells, fundamentals, technology and application, vol 4: fuel cell technology and applications, Part 2. John Wiley & Sons Ltd., p 1032
163. Menzler NH, Buchkremer HP, Ernst J, Kauert R, Ruska J, Stöver D, Stolz S (2007) Mater Sci Forum 539–543:1315
164. Stöver D, Buchkremer HP, Mai A, Menzler NH, Zahid M (2007) Mater Sci Forum 539–543:1367
165. Uhlenbruck S, Nédélec R, Buchkremer HP, Bram M, Menzler NH, Stöver D (2009) Proc. of the hydrogen and fuel cells 2009 conference, Vancouver, Canada, May 31–June 3, 2009, p A00296-1 (CD-ROM)
166. Heimann RB (2008) Plasma spray coating. Wiley–VCH, Weinheim, Germany
167. Pawlowski L (2008) The science and engineering of thermal spray coatings, 2nd edn. John Wiley & Sons Ltd., West Sussex, UK
168. Henne R (2007) J Therm Spray Technol 16:381
169. Lang M, Szabo P, Ilhan Z, Cinque S, Franco T, Schiller G (2007) Trans ASME 4:384
170. Syed AA, Ilhan Z, Arnold J, Schiller G, Weckmann H (2006) J Therm Spray Technol 15:617
171. Vaßen R, Hathiramani D, Mertens J, Haanappel VAC, Vinke IC (2007) Surf Coat Technol 202:499
172. Hathiramani D, Vaßen R, Stöver D, Damani RJ (2006) J Therm Spray Technol 15:593
173. Vaßen R, Stuke A, Stöver D (2009) J Therm Spray Technol 18:181
174. Zhang C, Liao H-L, Li W-J, Zhang G, Codded C, Li C-J, Li C-X, Ning X-J (2006) J Therm Spray Technol 15:598
175. Refke A, Barbezat G, Hawley D, Schmid RK (2004) Thermal spray 2004: advances in technology and application, proceedings, p 61
176. Mauer G, Vaßen R, Stöver D (2009) In: Marple BR, Hyland MM, Lau Y-C, Li C-J, Lima RS, Montavon G (eds) Proc. thermal spray 2009: expanding thermal spray performance to new markets and applications, Las Vegas, Nevada, USA, 04.–07.05.2009. ASM International, Materials Park, OH, USA, p 773
177. Hui R, Wang Z, Kesler O, Rose L, Jankovic J, Yick S, Maric R, Ghosh D (2007) J Power Sources 170:308
178. Wang Z, Oberste Berghaus J, Yick S, Decès-Petit C, Qu W, Hui R, Maric R, Ghosh D (2008) J Power Sources 76:90
179. Oberste Berghaus J, Legoux J-G, Moreau C, Hui R, Decès-Petit C, Qu W, Yick S, Wang Z, Maric R, Ghosh D (2008) J Therm Spray Technol 17(5–6):700
180. Grove WR (1842) Phil Mag 21:417
181. Grove WR (1852) Phil Trans R Soc 87:B142
182. Mahan JE (2000) Physical vapour deposition of thin films. John Wiley & Sons Inc., New York ISBN 0-471-33001-9, 115 ff
183. Jung HY, Hong K-S, Kim H, Park J-K, Son J-W, Kim J, Lee H-W, Lee J-H (2006) J Electrochem Soc 153:A961
184. Jordan Escalona N (2008) PhD thesis, ISBN 978-3-89336-565-4, 89 ff
185. Haanappel VAC, Smith M (2007) J Power Sources 171(2):169
186. Uhlenbruck S, Jordan N, Sebold D, Buchkremer HP, Haanappel VAC, Stöver D (2007) Thin Solid Films 515:4053
187. Nakagawa N, Yoshioka H, Kuroda C, Ishida M (1989) Solid State Ionics 35:249
188. Tsai T, Barnett SA (1995) J Electrochem Soc 142:3084

189. Pierson HO (1999) Handbook of chemical vapor deposition (CVD): principles, technology, and applications, 2nd edn. Noyes Publ., Norwich, USA. ISBN: 0815514328
190. Leskela M, Ritala M (2002) Thin Solid Films 409:138
191. Singhal SC (1999) In: Singhal SC, Dokiya M (eds) Proc. 6th SOFC (SOFC VI). The Electrochemical Society, Pennington, NJ, p 39
192. Pal UB, Singhal SC (1990) J Electrochem Soc 137(9):2937
193. De Souza RA, Kilner JA (1998) Solid State Ionics 106:175
194. Hammouche A, Siebert E, Hammou A, Keitz M (1991) J Electrochem Soc 138:1212
195. Fleig J (2003) Ann Rev Mater Res 33:361
196. Kenjo T, Nishiya M (1992) Solid State Ionics 57:295
197. Holtappels P, Bagger C (2002) J Eur Ceram Soc 22:41
198. Hart NT, Brandon NP, Day MJ, Shemilt JE (2001) J Mater Sci 36:1077. doi:10.1023/A:1004857104328
199. van Roosmalen JHM, Cordfunke EHP, Huijsmans JPP (1999) Solid State Ionics 66:285
200. Xu Q, Huang D, Chen W, Lee J, Kim B, Wang H, Yuan R (2004) Ceram Int 30:429
201. Mai A, Haanappel VAC, Uhlenbruck S, Tietz F, Stöver D (2005) Solid State Ionics 176:1341
202. Juhl M, Primdahl S, Manon C, Mogensen M (1996) J Power Sources 61:173
203. Haanappel VAC, Mertens J, Rutenbeck D, Tropartz C, Herzhof W, Sebold D, Tietz F (2005) J Power Sources 141:216
204. Radovic M, Lara-Curzio E (2004) Acta Mater 52:5747
205. Simwonis D, Thülen H, Dias FJ, Naoumidis A, Stöver D (1999) J Mater Proc Technol 92–93:107
206. Pratihar SK, Dassharma A, Maiti HS (2005) Mater Res Bull 40:1936
207. Han KR, Jeong Y, Lee H, Kim C-S (2007) Mater Lett 61:1242